FINNISH ROAD ADMINISTRATION

Leena Korkiala-Tanttu, Markku Juvankoski

HVS-NORDIC

The activity of the second period in Finland 2000 - 2003

Finnra Reports 45/2003

HVS-NORDIC

Swedish National Road Administration | Swedish National Road and Transport Research Institute | Technical Research Centre of Finland

Leena Korkiala-Tanttu, Markku Juvankoski

HVS-NORDIC

The activity of the second period in Finland 2000 - 2003

Finnra Reports 45/2003

Finnish Road Administration
Helsinki 2003

Pictures of the cover: Janne Sikiö. HVS-Nordic

ISSN 1457-9871
ISBN 951-803-126-6
TIEH 3200832E

Network publication pdf (www.tiehallinto.fi/julkaisut)
ISSN 1459-1553
ISBN 951-803-127-4
TIEH 3200832E-v

Multiprint Oy
Vaasa 2003

Publication sold by/available at:
Finnish Road Administration, publication sales
Telefax +358 (0) 204 22 2652
E-mail: julkaisumyynti@tiehallinto.fi

Finnish Road Administration
Opastinsilta 12 A
P.O.Box 33
FIN-00521 HELSINKI
Tel. exchange +358 (0) 204 22 150

Leena Korkiala-Tanttu, Markku Juvankoski: HVS-NORDIC. The activity of the second period in Finland 2000 – 2003. Helsinki 2003. Finnish Road Administration. Finnra Reports 45/2003. 55 p. + 5 p. app. ISSN 1457-9871, ISBN 951-803-126-6, TIEH 3200832E.

Keywords: accelerated pavement testing, instrumentation, road constructions, construction layers, properies, testing, test methods, bearing capacity, deterioration
Clasification: 32, 62

SUMMARY

An accelerated pavement testing facility, Heavy Vehicle Simulator (HVS) MARK IV, was bought from South Africa. It is owned on a 50/50 basis by Finland – the Technical Research Centre of Finland (VTT) and the Finnish National Road Administration (Finnra) – and Sweden – the Swedish Road and Transport Research Institute (VTI). HVS-NORDIC was used in Finland during 1997–98 (the first period) and 2000–02 (the second period) and in Sweden 1998–2000.

A six-year period of research collaboration from 1997 to 2003 was agreed upon. The co-operation was originally organised on three levels; steering, programme and operative groups. Since 2001, the programme and operative groups have been united in one group.

During the second period in Finland 18 tests were carried out in 5 different studies. The objectives in these studies were to examine the effects of reinforcement (steel grids, tests 11–13) and lightweight material (tests 14 and 15, expanded polystyrene EPS) on pavement behaviour. Tests 16–20 concentrated on the effect of steepness of sideslope on rutting (two slope inclinations + one without slope). The effect of the spring and overload on rutting (two load / two water table levels) were tested in tests 21–23. The effect of reinforcing the edge on a steep-sloped, rehabilitated pavement was studied in tests 24–29.

All the tested pavements represented low-volume roads and had thin (nominal thickness 50 mm) bituminous layers or rehabilitated layers. The common objective for all these second period tests was to study the permanent deformations of unbound layers.

The data from the tested constructions, observations and measurements were stored in the joint Finnish – Swedish database for all the partners to use. All the Finnish data from tests in the first and second HVS period in Finland have been checked, corrected, analysed and stored in the database.

The periodic report includes a summary of each test made during the period the HVS-NORDIC was located in Finland. In addition, the report includes a discussion of the experiences with the tests. The test plans and actual situation, and whether the testing went according to plan, are also discussed. The aim of the report is more informative than scientific.

FOREWORD

This is the second periodical report of HVS-NORDIC, the six-year joint Finnish-Swedish Research Programme on accelerated pavement testing. This report describes the activity of the second period in Finland.

The HVS-NORDIC research projects are part of the Finnish National Road Structures Research Programme, TPPT and Low-volume Road Research Programme, which have both been sponsored by the Finnish National Road Administration (Finnra). Finnra has also sponsored the Spring–Overload and Steep rehabilitated slope pavement tests together with Polyfelt Ges.m.b.H, Tammet Oy and Pintos Oy.

The members of the HVS team in VTT were Matti Huhtala, Jari Pihlajamäki, Pekka Halonen, Veikko Miettinen, Risto Alkio, Juhani Idman, Heikki Kangas, Seppo Saarelainen, Heikki Onninen, Jukka Elomaa, Janne Sikiö, Pekka Jauhiainen, Rainer Laaksonen, Leena Korkiala-Tanttu, Jouko Törnqvist and Markku Tuhola.

This report was edited by Leena Korkiala-Tanttu and Markku Juvankoski. Leena Korkiala-Tanttu and Markku Tuhola have been responsible for the HVS-NORDIC research projects in Finland since 2001. The projects have been carried out according to the guidelines of the HVS-NORDIC Programme group. The members of the Programme group also included Aarno Valkeisenmaki and Kari Lehtonen from Finnra, Rolf Magnusson, Hans Wirstam and Niclas Odermatt from SNRA, and Kent Gustafson and Leif G. Wiman from VTI.

Espoo, October, 2003

VTT Building and Transport

Finnish Road Administration

Contents

1 INTRODUCTION

1.1 Technical specifications of the machine

The machine is called HVS-NORDIC. The HVS Mark IV is a mobile full-scale accelerated pavement testing facility (Figure 1.1), whose loading is linear. It can be run over a short distance independently at walking speed, though in practice only at a specific test site. It can be moved as a semi-trailer over longer distances.

Figure 1.1. HVS-NORDIC accelerated pavement testing facility.

The HVS-NORDIC has a heating/cooling system and, thus, the temperature can be kept constant. The air temperature inside the heating/cooling box is controlled in order to keep the pavement temperature constant. The selected standard temperature of the bituminous layers was +10°C.

The main technical characteristics are: length 23 m, width 3.5 m, height 4.2 m and weight 46 t. The loading wheels are dual or single; the standard dual wheel type is 295/80R22.5 and the wide base wheel type is 425/65R22.5. Loading can be uni- or bi-directional, and the lateral movement is 0.75 m. The wheel load is 20–110 kN (corresponding axle loads 40–220 kN) at speeds up to 15 km/h. The number of loadings is 25,000 in 24 hours (including daily maintenance). The loading of the HVS-NORDIC can be varied dynamically ± 20%.

1.2 Test site

The test site is located a few hundred metres from the VTT office. The site includes two test basins. One test basin is made of concrete; the walls have thermal insulation and there is complete water table regulation (Fig 1.2). Its length is 36 m including a 16-m-long slope and its depth is 2.5 m and width 4 m at the top and 3 m at the bottom. Two or three test pavements can be constructed in the test basin.

Figure 1.2. Concrete basin in Otaniemi.

The second test basin is parallel to the first one. It is excavated mainly in rock and has complete water table regulation. It is roughly the same size as test basin no. 1. There is a tent providing protection from the elements above the basin.

1.3 Instrumentation

The objective of the instrumentation was to monitor and measure deformations and changes in moisture and temperature occurring in the structure. Structural deformations, earth pressures and the water content of the layers were measured during loading. The responses recorded in the measurements were both dynamic and static.

Some of the instruments were installed after the test structure was built. Sensors for measuring earth pressure and displacements were installed during the construction. The sensors were calibrated and installed carefully following instrument-specific instructions.

Post-construction instrumentation consisted of instruments and their installation tubes measuring temperature, water content in the structures and asphalt deflection. Asphalt deflection was measured with an accelerometer, which was installed in each structure immediately prior to the start of the test.

Deflection before, during and after the test was measured by a falling weight deflectometer.

1.4 Test procedure

The tests were started first with a preloading in order to relax possible residual stresses and cause some post-compaction. This was done with a small wheel load, usually 30 kN and with specific lateral distribution.

After the preloading, zero measurements were made in order to measure the initial state of construction. They included a considerable number of response measurements: strain, stress and deflection measurements at different wheel loads, tyre inflation pressures, lateral positions and temperatures. Both wide base tyre and dual tyres were used. The same measurements were repeated later during the test but not so comprehensively.

Transversal profiles were measured at three to five locations with a laser profilograph constructed by VTI for the HVS-NORDIC. Rutting was expressed as a mean value of rut depths in the middle of the wheel path, where the largest rut depth can normally be obtained.

The cracks were drawn on paper and were also photographed.

1.5 Database

The database includes all the information on test fields, pavement structures, sensors and materials, as well as loading parameters. Environment data, as well as profile and FWD results, are in their own tables. The driving history is complete only in the HVS files and only selected information relevant to research has been saved in the joint database. Measurement signals have been saved in their own signal files. Only the top values, etc., which have been used in data analysis, have been stored in the joint database. The data of the structures and response measurements are in the joint database.

1.6 Test programme

REFLEX AND EPS TESTS (11–15)

The structures of tests 11, 12 and 13 formed part of the Task 4 ”Full Scale Accelerated Tests” in the EU REFLEX project /Pihlajamäki *et al.* 2002/. The main objective of REFLEX was to develop new technology for road construction and rehabilitation. The idea was to use steel fabric reinforcement in asphalt roads in order to make road structures more cost effective by improving the lifetime of new roads and by developing an optimal rehabilitation method for existing roads. The Task 4 tests were planned based on comments and recommendations by Reflex project members.

The Finnish structures tested the increase of the bearing capacity of a reinforced pavement. The steel grid was installed in the unbound granular base course in the structures. The reinforced structures of tests 11 and 12 were similar to each other except for the steel grid dimensions of the bars and openings.

The structure of test 13 was an unreinforced reference structure similar to tests 11 and 12. Its structure was similar to tests 11 and 12.

The objective of these tests was to simulate the number of load applications reinforced structures can carry under controlled conditions and compared with conventional unreinforced structures.

The structures of tests 14 and 15 were built in the same test basin as structures 11–13. These structures were otherwise similiar to structures 11–13, except that they also included lightweight material, expanded polystyrene (EPS) underlying the base course /Elomaa 2002/. Test structure 15 also included a steel grid similiar to test 12. The purpose of these tests was to define the mechanical properties and functioning of EPS and the behaviour of structures, deformations and deterioration, in cyclic loading.

The pavements of tests 11–15 had thin bituminous layers and they are for low-volume roads. The testing was carried out in the winter of 2001.

LOW-VOLUME ROAD TESTS (16–20)

The structures of tests 16–20 were also low-volume road pavements. These tests were done in a study *"Effect of steepness of sideslope on rutting"* /Korkiala-Tanttu *et al.* 2003a/. It was part of a research project to develop economical maintenance of low-volume roads and focused on the behaviour of roads with low bearing capacity. The Low-volume road structure project was realised through co-operation between the University of Oulu and VTT Building and Transport under a steering body consisting also of Finnish Road Administration (Finnra) and Finnish Road Enterprise representatives.

These tests were special in that the test sections included slopes. Tests 16 and 17 formed the first test section without a slope; test 18 formed the second section with a 1:3 slope and tests 19 and 20 formed the third section with a 1:1.5 slope.

There were only minor differences between test structures 16 and 17 and between test structures 19 and 20. The difference was that the beginning of structure 16 and the end of structure 20 included a bi-component geotextile 3 m wide placed over the subgrade clay, while a conventional geotextile was used in the other parts /Korkiala-Tanttu *et al.* 2002/. In all other respects the structures were identical and they were also tested identically. At the end of the tests, the water level was raised from a little below the subgrade level to the top of the gravel layer and finally to the centre of the crushed rock. The pavement response, due to moving the wheel load with several offsets, was measured and finally the pavement performance was evaluated with accelerated testing. The test sections were constructed and instrumented in autumn 2000. The area was insulated during the winter and the test was performed one year later.

The objective of tests 16–20 was to study the influence of the road cross-section and edge on the structural strength and permanent deformations of low-volume roads. The purpose of the test results was to verify design methods and calculation models.

SPRING–OVERLOAD TESTS (21–23)

The structures of tests 21–23 were also low-volume pavements. These tests were carried out in a study *"Effect of spring and overload on the rutting of a low-volume road"* /Korkiala-Tanttu *et al*. 2003b/ financed by Finnra. This study complemented the Low-volume road structures project. The study was carried out by VTT Building and Transport under the supervision of Finnra according to a research plan.

The aim of the study was to acquire basic information on the behaviour of road structures with low bearing capacity. The study also aimed at discovering whether the fourth power rule applies, as well as the effect of spring on low-volume roads under a Heavy Vehicle Simulator (HVS) load imitating the passing of a lorry. The testing was carried out in the spring of 2002.

In tests 21–23 all the structures were uniform, but there were differences between the wheel loads applied and the water table levels were also different.

REHABILITATED PAVEMENT WITH STEEP SLOPE (24–29)

The structures of tests 24–29 were also low-volume road structures. The research *Reinforcement of the edge of a steep-sloped pavement* /Korkiala-Tanttu *et al.* 2003c/ studied what effect the reinforcement grid used in the rehabilitation of rutted structures has on decelerating rutting in structures with low bearing capacity edges. The second aim was to ascertain whether different reinforcement grids differed in decelerating rutting. The research was financed by Finnra, Tammet Oy, Pintos Oy and Polyfelt Ges.m.b.H.

The Low-volume road test structures were rehabilitated and a steep sideslope of 1:1.5 was constructed. The rehabilitated structures (24–29) had two unreinforced reference structures, one with fibreglass geotextile and three with two different steel grids. The loading programme followed the same pattern as in the Low-volume road test, except that the number of the passes was doubled.

1.7 Reporting of the research programme

The research programme has been reported at four different levels. The reporting focused on different aspects.

The **Weekly report** is information about running the tests. It includes the pavement structure, loading parameters, figures of the number of loadings *vs*. time, and rutting/cracks *vs*. the number of loadings. It also includes information about problems. It was sent every week by e-mail to the "HVS-NORDIC group".

The **Periodic report** includes a summary of each test made during the period the HVS-NORDIC was located in Finland or Sweden. The report provides an update of the database. In addition, the report includes a discussion of the experiences with the HVS-NORDIC, and its ability to test road distress. The test plans and actual situation, and whether the testing went ac-

cording to plan, are also discussed. The aim of the report is more informative than scientific.

The **Research report** is a conventional (scientific) research report. Ideally, it includes several similar tests, like thawing tests, laboratory tests, etc. It is a compilation of similar kinds of tests.

The **Conference papers** are information about the research programme. Depending on the conference subjects, the papers can be written by individual members of the group. The target is to market and inform about HVS-NORDIC.

2 DESCRIPTION OF THE TESTS

2.1 Tests 11–13, reinforced structures (REFLEX03)

Three full-scale accelerated tests were performed within REFLEX Task 4, two in Sweden and one in Finland. The Finnish test (Reflex 03) included two different steel reinforced sections (tests 11 and 12) and additionally one section (test 13) was made as a reference without reinforcements (Figure 2.1). The Finnish test structures were constructed using ordinary road construction machines in the rock test basin in Otaniemi.

In these structures the surface layer was 50 mm typical Finnish asphalt concrete AC16/125, bitumen penetration 80. The granular base course was crushed rock 0–32 mm. The subgrade was fine-sand.

Steel grid was installed in the unbound granular base course, 50 mm above the sand interface. The steel grid in the first section had a pitch size of #75 mm and a bar dimension of 5 mm. The dimensions of the steel grid in the second section were #150 mm and 6 mm, respectively.

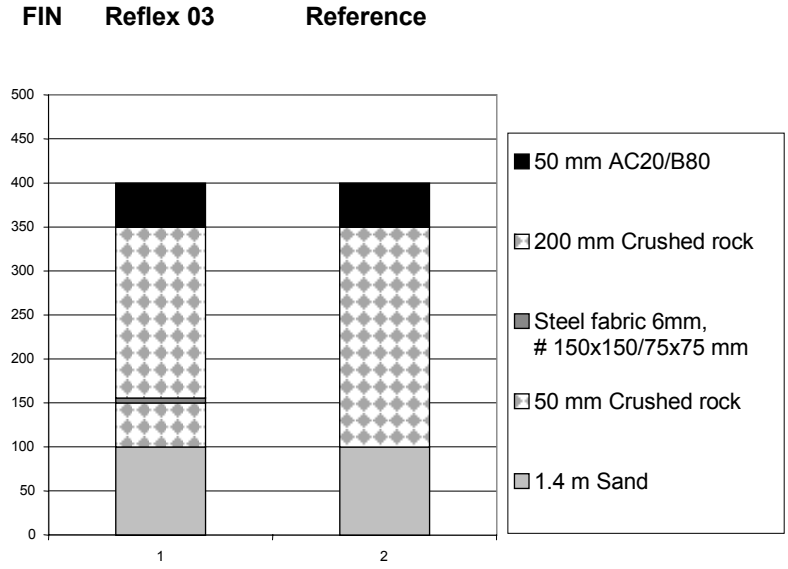

Figure 2.1. Test structure, Reflex 03 /Pihjalamäki et al. 2002/.

The test structure (called Reflex 03) was instrumented in the loading centreline as shown in Figure 2.2. As can be seen in Figure 2.2 the following response parameters were measured during the test:

- surface deflection
- longitudinal and transverse strain at the bottom of the AC layer
- longitudinal and transverse strain in the steel grid
- vertical stress in the sand subgrade
- vertical strain in the sand subgrade

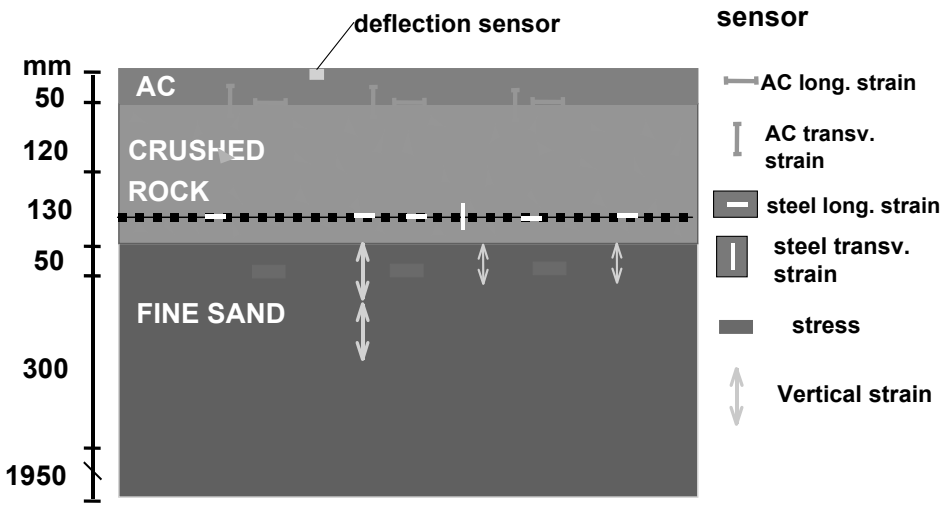

Figure 2.2. Longitudinal section, Reflex 03. Instrumentation in centreline /Pihlajamäki et al. *2002/.*

In all of the tests, the pavement temperature was also measured on the top, in the middle and at the bottom of the bituminous layer.

Before and during the tests, the rut depths were calculated from transverse profiles measured at 6 fixed sections with a laser profilometer. Crack inspection was done regularly and when cracks appeared their lengths were measured and their places documented. The results from the tests were primarily the development of rut depths and cracks versus the number of load repetitions.

The rut depth development is presented in Figure 2.3. It can be seen that both reinforced test sections have about the same rutting behaviour. The rutting of the reference section is significantly faster. The reinforced sections tolerate 50–100% (depending on the rutting level) more load repetitions than the (unreinforced) reference structure at the same rut level.

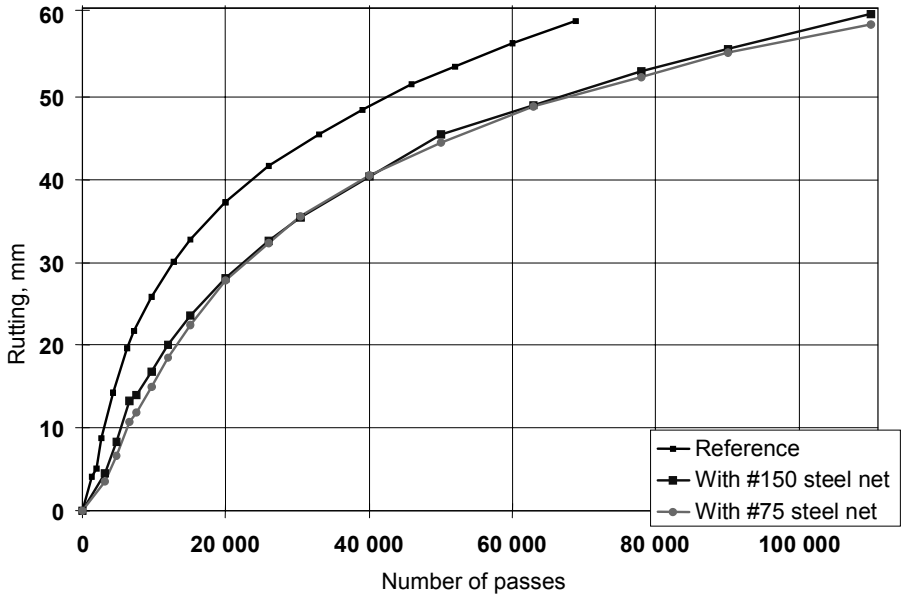

Figure 2.3. Rut depth development in Reflex03 test /Pihlajamäki et al*. 2002/.*

2.2 Tests 14 and 15, lightweight material, expanded polystyrene (EPS)

Test structures 14 and 15 were constructed in the same test basin excavated in rock as the REFLEX structures presented above. The test structures were constructed of homogenous layers of equal thickness. The subgrade consisted of 1.5 m of sand. The sand layer was topped by a layer of expanded polystyrene (EPS) lightweight fill in 200 x 1200 x 5 000 mm blocks. An application class 2 filter cloth was installed on top of the EPS layer. The unbound pavement consisted of a 450 mm layer of crushed rock (Teisko crushed rock # 0–60 mm). The surface layer consisted of a 50 mm layer of asphalt concrete (AC, B-80, 16/125). Half of the structure was reinforced with a steel grid, the reinforced structure being number 14 and the unreinforced number 15. The grid was installed in the crushed rock layer 100 mm above the top of the EPS. The spot-welded grid was made of 6/6 mm ribbed bars and the size of the openings was 150x150 mm^2.

The test was part of the EPStress programme, which studies the load capacity of an EPS layer. The purpose of the tests was to determine the mechanical properties and performance of EPS in cyclic loading in order to design the load capacity. The EPS lightweight fill was designed so that the load repetitions necessary for the failure of the structure could be achieved within two weeks of beginning the loading. Measuring instruments installed in the test structures aimed at providing information on the loads the EPS material was subject to and deformations in the materials. In addition, surface layer and pavement deformation and distress under traffic load was investigated /Elomaa 2002/.

Figure 2.4 is a profile drawing of the test structure. The Figure shows the measuring instruments installed in the structure, EPS blocks and the division of the structure into one reinforced with a steel grid and an unreinforced one.

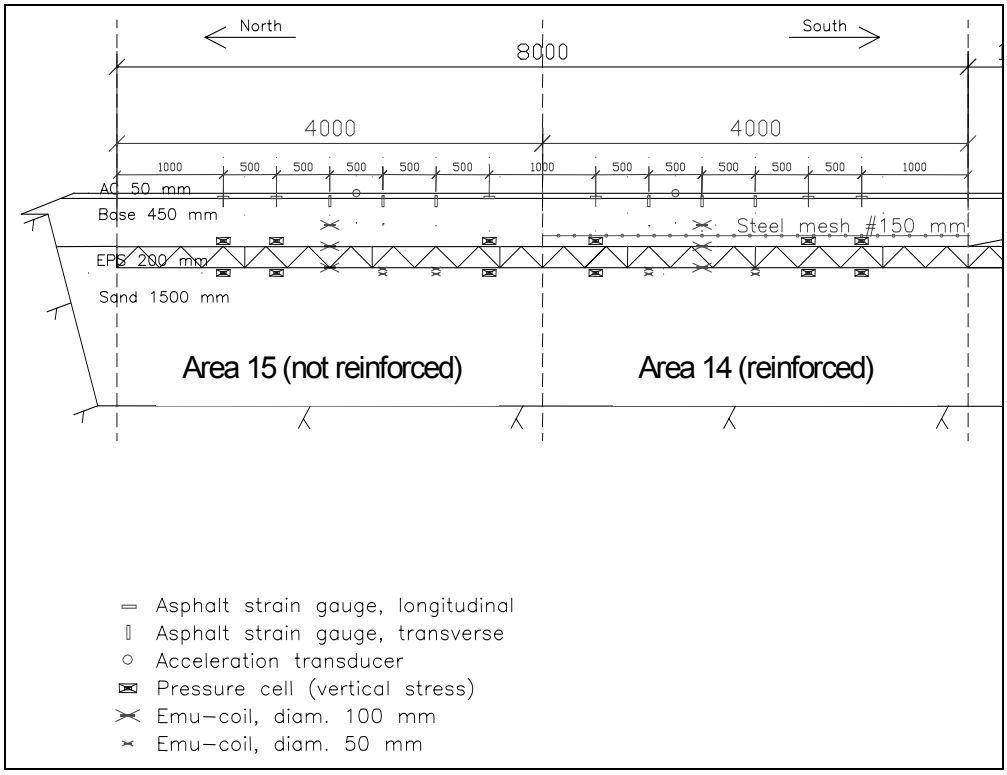

Figure 2.4. Longitudinal profile of the test structure and the measuring instruments installed in it /Elomaa 2002/.

The rutting of the structure's surface layer was measured with a laser profilometer. The profiles were measured transversely in relation to the wheel's path at 0.5 m intervals on six measuring lines on both areas.

The test area reinforced with a steel grid and the unreinforced one rutted nearly equally during preloading (10.6 mm and 11.1 mm). This lends support to the idea that a steel grid has little effect on the bearing capacity and rutting in the early stages of loading. Only after the structure had compacted sufficiently did the grid begin to improve the structure's bearing capacity and, thus, slow down rutting. Figures 2.5 and 2.6 show the development of the deepest rut in relation to load repetitions on all the measuring lines. The Figures also show the average depth of the deepest rut in the area.

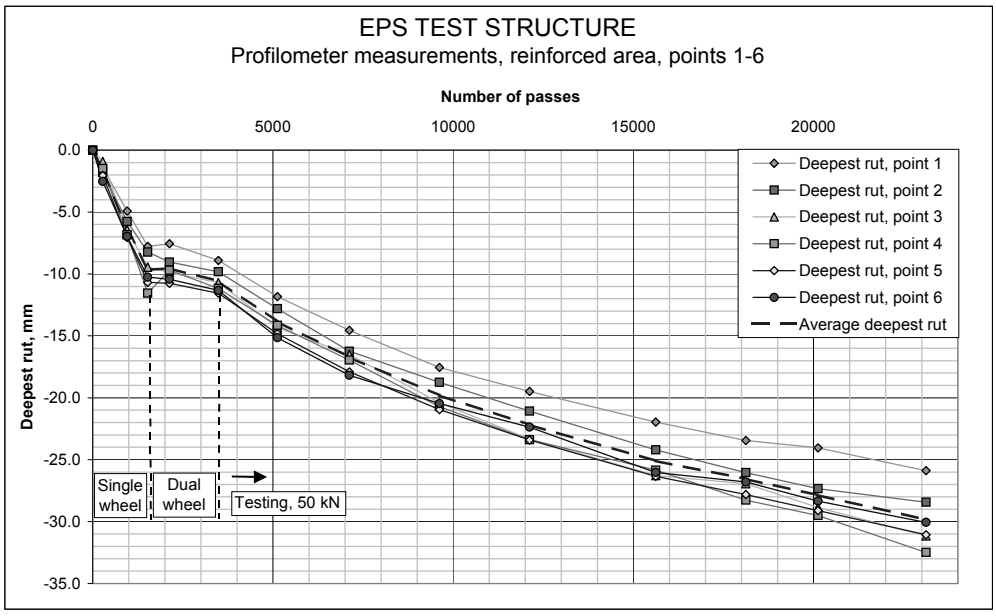

Figure 2.5 Rutting of the surface layer in relation to the number of passes according to the measuring lines on the structure reinforced with a steel grid (test 14) /Elomaa 2002/.

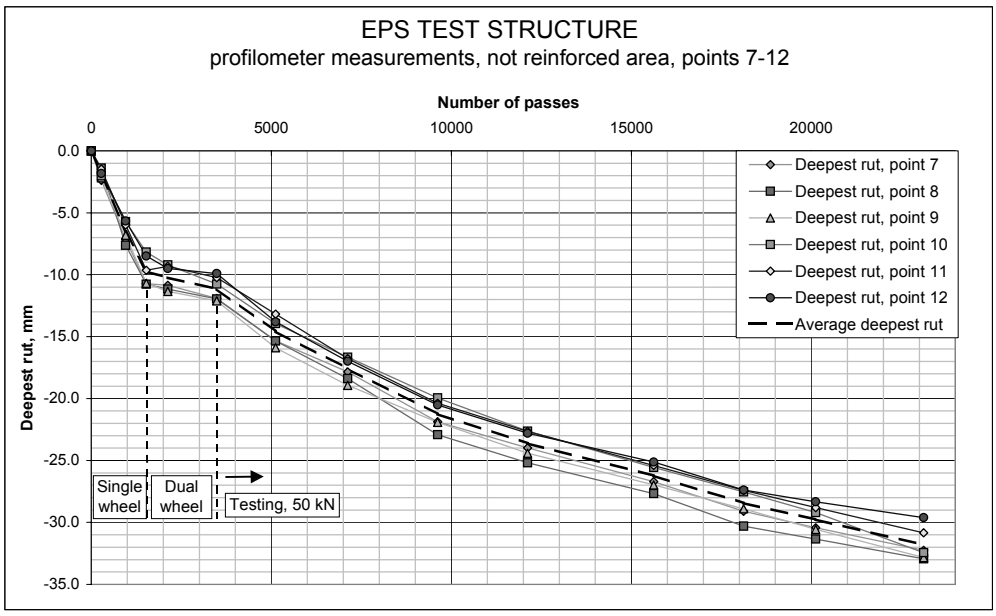

Figure 2.6 Rutting of the surface layer in relation to the number of passes according to the measuring lines on the unreinforced structure (test 15) /Elomaa 2002/.

2.3 Tests 16–20, sloped structures

Three different low-volume structures (Figure 2.7) were constructed in the concrete test basin: one without a slope (tests 16 and 17), one with a gentle slope (1:3) (test 18) and one with a steep slope (1:1.5) (tests 19 and 20). Before moving the HVS to the test site, the slopes were covered with filter cloth and filled with gravel to facilitate the move, after which the slopes were dug open again /Korkiala-Tanttu *et al* 2003a/.

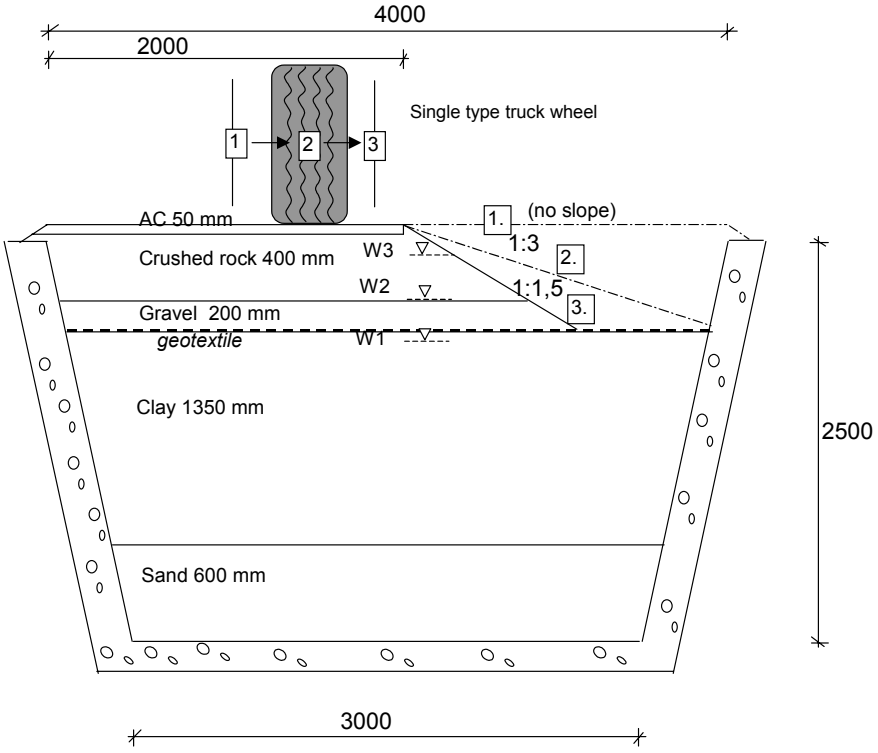

Figure 2.7. Cross-section of low-volume structure (no slope, 1:3 and 1:1.5 slopes) /Korkiala-Tanttu et al*. 2003a/.*

The materials of the structure and the thickness of the layers were identical on all the load sections. The subgrade of the structure consisted of the existing subsoil drainage and a clay layer. Total thickness of the pavement above the clay was approximately 640 mm (Figure 2.7). An application class 3 filter cloth was fitted over it. A 3-metre wide bi-component geotextile, the functioning of which was the subject of a separate report /Korkiala-Tanttu *et al*. 2002/ was fitted to the ends of the basin.

The unbound pavement consisted of a 200 mm layer of compacted, sandy gravel as subbase and an upper layer (base course) of 400 mm of crushed rock. The lean clay came from Lahti, the sandy gravel (# 0–50 mm) from Hyvinkää and the crushed rock (# 0–32 mm) from Teisko. The subbase was applied so that it could also be compacted in the slope structures for the whole width of the loading area. The overlay consisted of 40 mm asphalt concrete (AC16/100) with a grain size of 0–16 mm, and bitumen B70/100.

The length of each section was 8 m, with the load parameters and conditions remaining constant on 6 m (Figure 2.8).

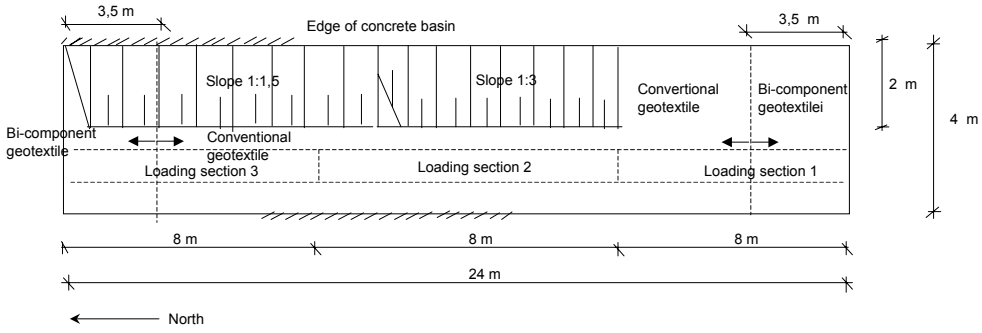

Figure 2.8. Map of the structure /Korkiala-Tanttu et al*. 2003a/.*

The construction work was carried out in autumn 2000 and the test structure was then protected for the winter by insulating it. The actual testing began in June 2001.

Test structures were instrumented according to a separate instrumentation plan. Sensors for volumetric water content, earth pressure, pore pressure and displacements (Emu-Coil sensors and settlement profile tubes) were installed during the construction. Post-construction instrumentation consisted of instruments including installation tubes for measuring temperature, water content in the structures and variations in the pore pressure, as well as asphalt deflection and slope displacement.

The basic water table level during the tests was +15.70. In the final phases of loading each test, the ground water table was elevated to the level of the top of the gravel layer (W2) at the minimum, and on sections with a gentle or steep slope, also to the layer of crushed rock (W3). The variation in the ground water level and the loads on each section are presented in Figure 2.9 (see also Figure 2.7).

The development of the rut depth was measured during the tests with a profilometer. Distress surveys were made also on the top of the surface layer immediately after the first cracks appeared. Figure 2.10 shows the development of the rut depth for all three structures. As can already be seen in Figure 2.10, the changes in the water table level had a remarkable effect on the results. The gravel included fine-grained particles, so the capillary rise of the water and its influence was evident.

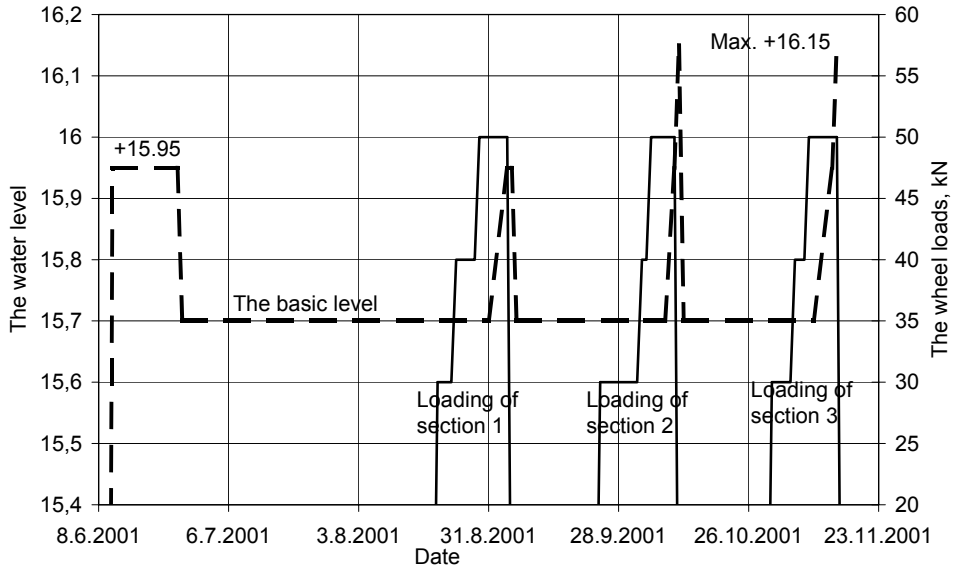

Figure 2.9. Ground water level and the loading times of the different sections /Korkiala-Tanttu 2003a/.

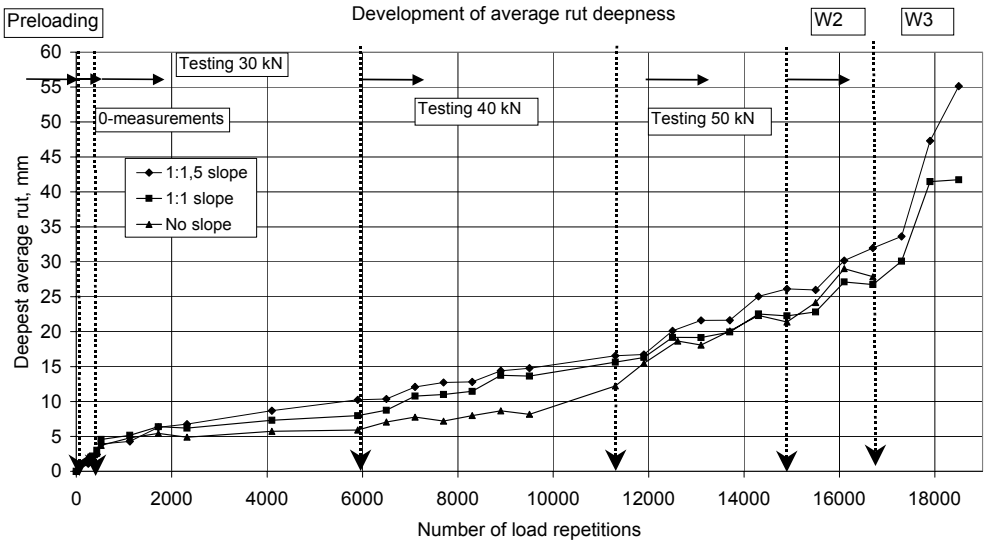

Figure 2.10. Development of rut depth as a function of load /Korkiala-Tanttu et al*. 2003a/.*

2.4 Tests 21–23, spring and overload

The test structure for tests 21–23 was built in the rock basin. The structure was the same on all the sections to be tested. The total thickness of the pavements was 500 mm. The structure chosen corresponded to the pavements of low-volume roads /Korkiala-Tanttu *et al.* 2003b/.

Before constructing the test structure, old test structures (tests 11–15) were removed from the basin as far as the surface of the subgrade layer. Thus, the subgrade consisted of fine to medium sand that had been in the bottom of the previous test structure.

The subbase consisted of low-grade crushed gravel with grain size 0–35 mm. The thickness of the layer was 250 mm. The crushed gravel was brought from Jutikkala. The base course was made of crushed rock from Teisko, with a grain size of 0–32 mm and a thickness of 200 mm. The surface layer consisted of a 50 mm layer of asphalt concrete (AC16/125, B70/100). The cross-section of the structure is shown in Figure 2.11.

The test structure was constructed in January and February 2002. Due to winter working conditions, the materials in the base course and in the lower layer of the pavement were not watered during compaction.

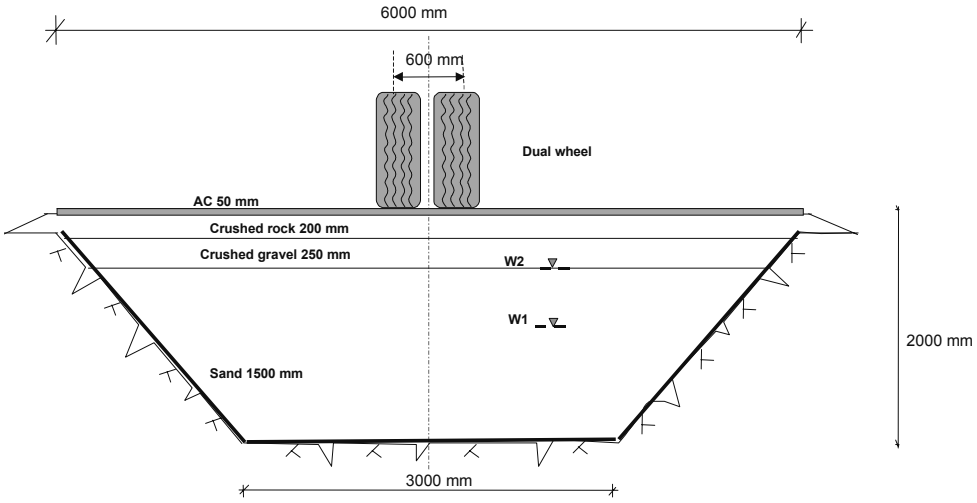

Figure 2.11. Cross-section of the structure /Korkiala-Tanttu et al*. 2003b/.*

The objective of the instrumentation of the structure was to monitor and measure deformations and changes in moisture and temperature occurring in the structure. Structural deformations, earth pressures and the water content of the layers were measured during loading. The responses recorded in the measurements were both dynamic and static.

Sensors for measuring earth pressure and displacements were installed during the construction. The sensors were calibrated and installed carefully following instrument-specific instructions. The test structures were also equipped with instruments related to a deformation project (settlement profile tubes and aluminium foil). Post-construction instrumentation consisted of instruments and their installation tubes measuring temperature, water content in the structures and asphalt deflection. Asphalt deflection was measured with an accelerometer, which was installed in each structure immediately prior to the start of the test. Figure 2.12 shows the numbering of the test sections, loads and water table levels.

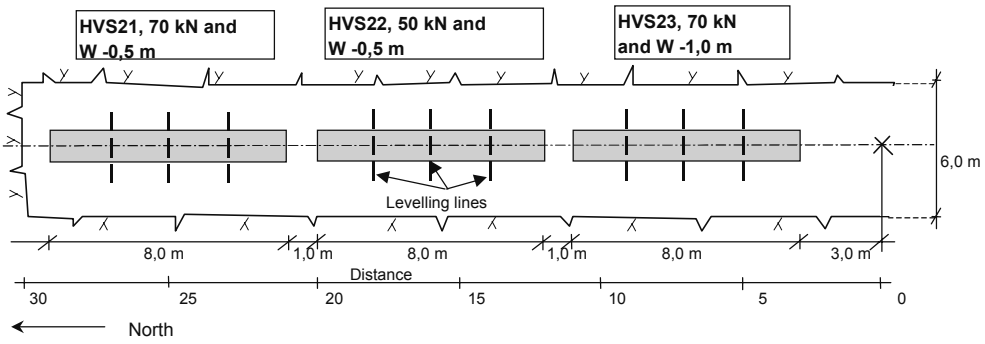

Figure 2.12. Dimensions and numbering of test sections /Korkiala-Tanttu et al. *2003b/.*

The basic water table level during the first two tests was the bottom of the subbase (W2). During the last test (23), the water table level was lowered to approximately 1000 mm from the top of the surface layer (W1).

Testing began at the beginning of March 2002. The structures were tested in the following order: structure 22 (50 kN, W2), structure 21 (70 kN, W2) and finally structure 23 (70 kN, W1). Figure 2.13 shows the loading schedule and the changes in the water table level. See also Figure 2.8 for water table level.

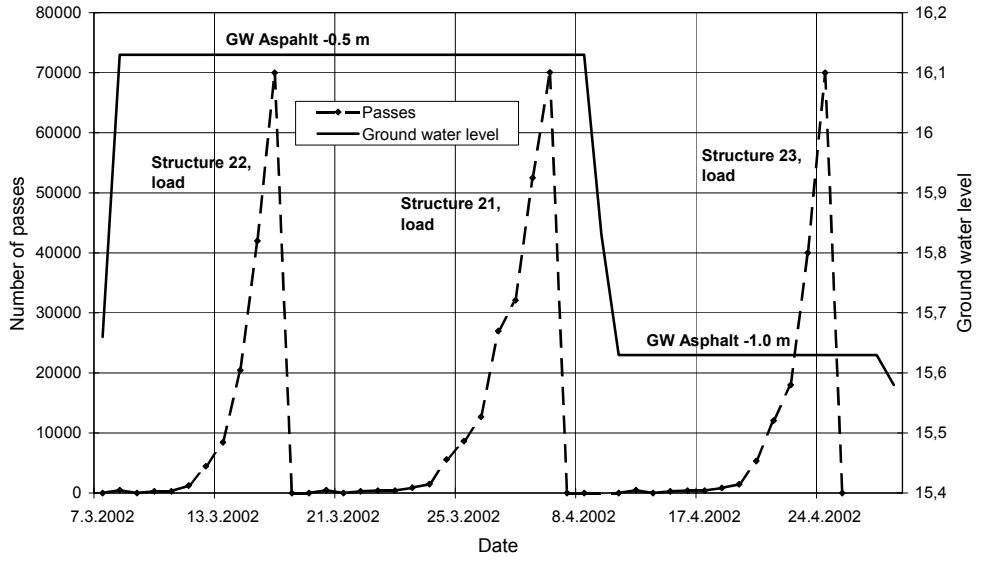

Figure 2.13. Loading the structures and level of ground water measured in the pilot well /Korkiala-Tanttu et al*. 2003b/.*

The rutting of the structures' surfaces was monitored with profilometer measurements (levelling lines see Figure 2.12). Because there were some differences in the thickness of the asphalt layer, the measured rut depths were converted in relation to the thickness (see details in Chapter 3). These

converted rut depths and a calculated rut depth for an imaginary structure with a load of 50 kN and ground water level at -1.0 m are shown in Figure 2.14.

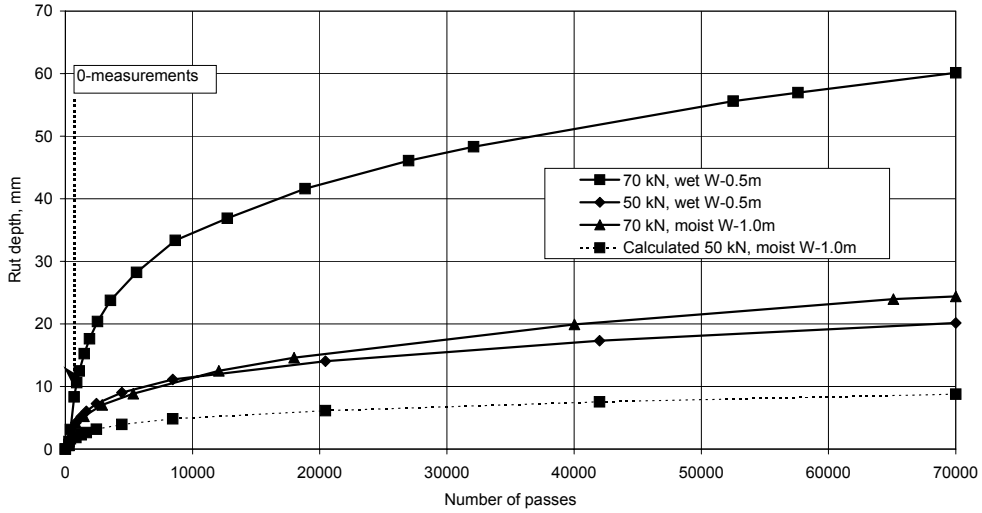

Figure 2.14. Estimated rutting of different structures in relation to the number of passes /Korkiala-Tanttu et al. *2003b/.*

2.5 Tests 24–29, rehabilitated steep slope structure

Structures 16–20 that had become rutted and otherwise damaged in the tests for the Low-volume roads project were used as the base for the tested structures in this study. The structures were one with no slope, one with a gentle slope (1:3) and one with a steep slope (1:1.5). The previous tests studied the effect of slope steepness and position on rutting. Due to differences in the cross-sections, the structures had clearly rutted differently. The deepest ruts were approximately 55 mm (steep slope) and the shallowest approximately 28 mm (no slope).

For this study, every 8-metre long test structure was divided into two 4-metre strips, which could be directly compared. In order to obtain comparable results between the different structures, two identical pairs of structures were tested, each with steel grid 1 and an unreinforced reference structure. These structures were numbers 24 and 25, and 28 and 29. The middle structures were reinforced with another type of steel grid and fibreglass reinforcement. The reinforcements used, the positions of the structures – also in relation to the old structures – and their numbering are presented in Figure 2.15.

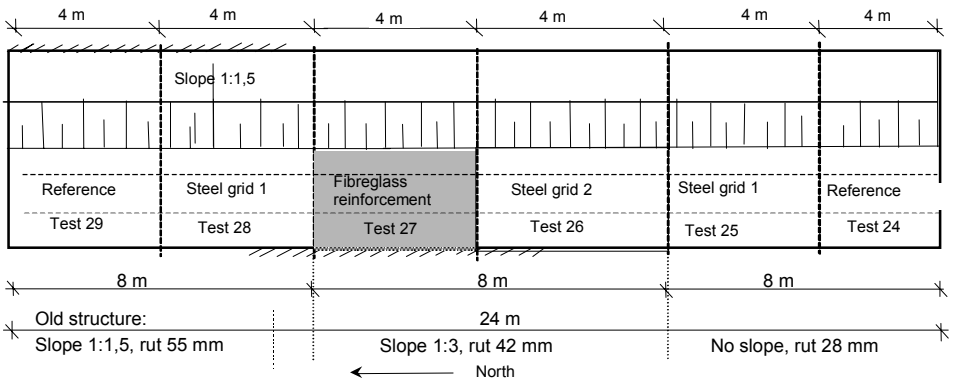

Figure 2.15. Test structures and their state before rehabilitation.

The standard cross-section of the test structures is presented in Figure 2.16. After the first phase tests were completed, the structures, which had rutted during the loading, remained outside unprotected over the winter 2001–2002. The structures had visibly rutted in the first phase of the study and cracks could be observed. The cracks were mainly short and narrow, only the inside edge of the rut in the structure with the steep slope (structure 28–29) showed a crack for the entire length of the rut.

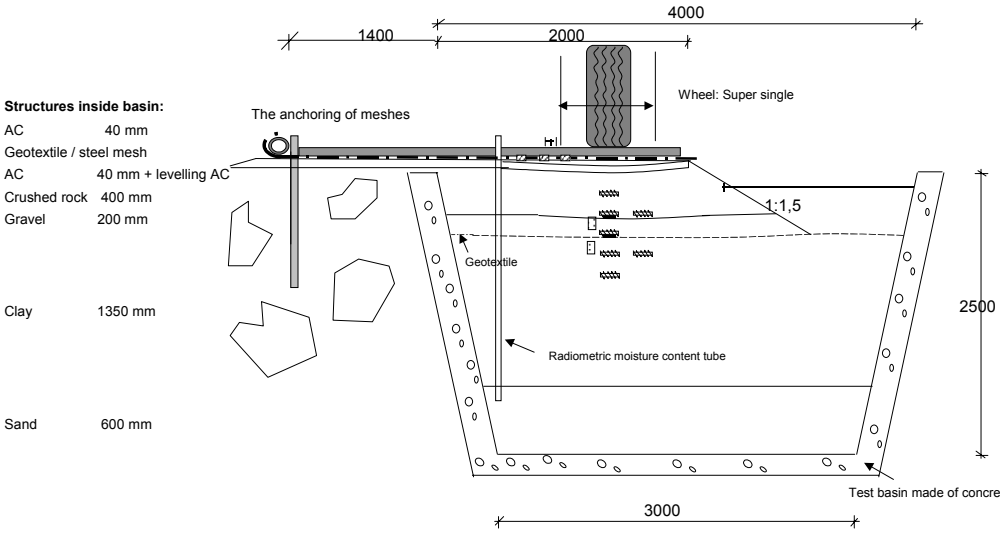

Figure 2.16. Cross-section of the test structure with the steep slope.

The structures were rehabilitated by first levelling out the rut with levelling mix and then installing the reinforcements on the levelled surface. The steel grids used were B500H-5/6-200/150 and B500H-5/8-200/150, which differed from each other only by the diameter of the bar (6 mm – 8 mm). The reinforcements were anchored around a 36 mm diameter steel tube outside the basin (Figure 2.16). The purpose of the anchoring was to simulate the anchoring effect caused by the weight of the other lane when a full-width steel grid is installed on a 7 m wide normal road. One edge of the steel grid was bent at the factory to fit the steel tube. The steel grids were instrumented

with strain gauges, which measured stress forming in the transverse steel bar.

The fibreglass reinforcement chosen was Polyfelt PGM-G100/100 supplied by Polyfelt Ges.m.b.H. It is designed for road construction and its tensile strength in both directions is 100 kN/m. This strength corresponds roughly to the strength of the steel grids. The fibreglass geotextile was glued on both sides with bitumen emulsion according to the manufacturer's instructions. The fibreglass reinforcement was also anchored to the steel tube by winding the reinforcement tightly around the tube and doubling the extra material for 400 mm. The reinforcement was kept tight during the spreading of the bitumen emulsion and the asphalt layer to avoid folds.

A 40 mm layer of asphalt was finally spread over the reinforcements. A steep (1:1.5) slope was dug alongside the test structure after the heavy vehicle simulator was moved to the site, but before the loading began.

The test was organised mainly like the tests in the Low-volume roads project. Prior to actual testing, the water table level was elevated to the bottom of the subbase (W2 = +15.95) for a few days. After this, it was lowered to the basic level during testing (W1 = +15.70, 50 mm below the surface of the subgrade). Falling weight deflectometer measurements were conducted during the higher level of the ground water. During the 50 kN load in the loading of each section, the ground water table was elevated to the top of the gravel layer (W2 +15.95), and also to the layer of crushed rock (W3 +16.15).

All the structures were loaded according to the same loading programme. The loading programme resembled the loading programme of the Low-volume road study, but the number of passes was doubled. The test wheel was a Super Single wheel and the tyre pressure on all the wheel loads was 700 kPa. The loading distribution was the normal distribution, the width of which was ± 300 mm from the centreline. This loading distribution differed from the one used in the Low-volume road study, which used three loading lines at 300 mm intervals, all loaded identically.

The states of the structures differed after the rehabilitation because the structure that had become the most rutted in the first phase of tests had the thickest new surface layer. However, falling weight deflectometer measurements before and after the test did not show significant differences between the different structures. The different reinforcements did not seem to have a significant effect on the bearing capacity values determined with the falling weight deflectometer. The structure pairs with greater differences in rut depth, however, also yielded greater differences in bearing capacity.

The rutting and distress of the structures were monitored during the test. However, no distress was perceived at the end of the test, so the comparisons are only made for rutting. No differences were perceived in the performance of the different reinforcements.

The reinforced structure in pair 24–25 (former structure with no slope) rutted approximately 25–30% slower than the corresponding unreinforced structure, while the reinforced structure in pair 28–29 (former 1:1.5 slope) rutted 55–60% slower than the unreinforced structure. The rutting of the reinforced structures in pair 26–27 falls between these values. The deceleration of rut-

ting in structures 24–25 corresponds to approximately a 40–50% extension of service life. Correspondingly, the deceleration in structures 28–29 means approximately 130–190% longer service life. The great differences in structure performance can be explained not only by deformations already existing in the structures, but also by the fact that the thickness of the pavements differed by approximately 30%. Other factors could include variation in how the surface layers adhered to each other and variation associated with the building process.

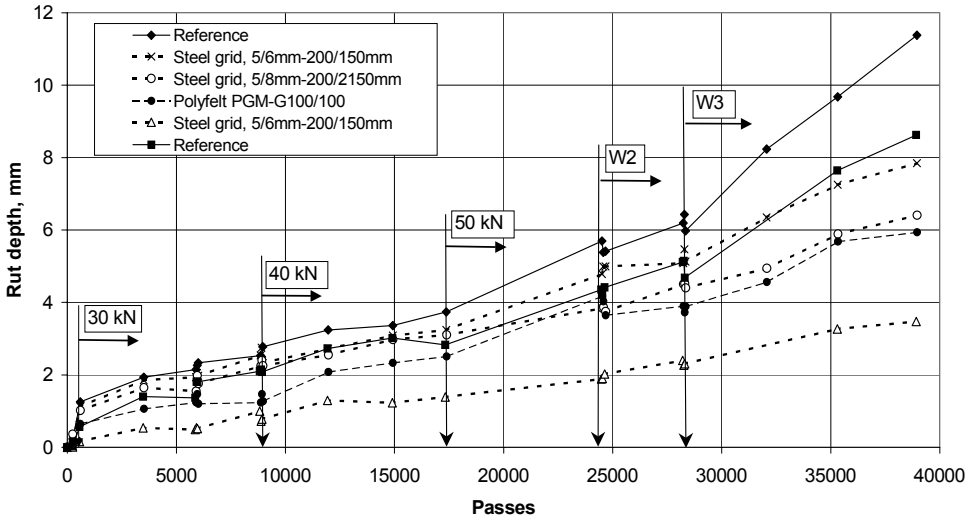

Figure 2.17. Rutting of the surfaces of the structures

3 EVALUATION OF RESULTS

The results and parameters of each test made in Finland during the second period are briefly presented in Appendix 1 at the end of this report.

3.1 The effect of reinforcements in unbound base course

The structures of tests 11, 12 and 13 formed part of Task 4 ”Full Scale Accelerated Tests” in the EU REFLEX project /Pihlajamäki *et al.* 2002/. The objective of these tests was to simulate the number of load applications reinforced structures can carry under controlled conditions and compared with conventional unreinforced structures. Test parameters are shown in Appendix 1. The results from the main tests were primarily the development of rut depths and cracks versus the number of load repetitions.

The rut depth development is already presented in Chapter 2. Both reinforced test sections had about the same rutting behaviour. Rutting of the reference section was significantly faster. Reinforced sections tolerated 50–100% (depending on rutting level) more load repetitions than the (unreinforced) reference structure at the same rut level.

The crack propagation is presented in Figure 3.1. The reinforced structure with a small pitch size seems to have better resistance to cracking than that with a larger pitch size. However, the reference structure without reinforcement has about the same performance as the steel reinforced structures.

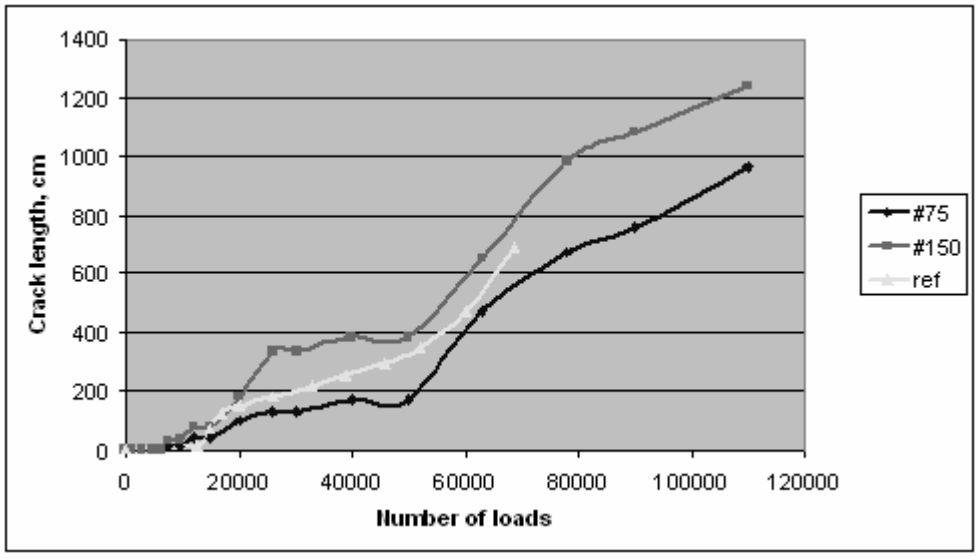

Figure 3.1. Crack propagation in the Finnish bearing capacity test, Reflex03 /Pihlajamäki et al*. 2002/.*

3.2 The effect of lightweight material (expanded polystyrene, EPS)

The purpose of test structures 14 and 15 was to determine the mechanical properties and performance of EPS in cyclic loading for designing the load capacity. Measuring instruments installed in the test structures aimed at providing information on the stresses the EPS material was subject to and deformations in the material. In addition, surface layer and pavement deformation and distress under traffic load was investigated.

The rutting structure by structure is presented above in Chapter 2.

The development of rutting on the centreline of the structure's surface in relation to the number of passes is presented in Figure 3.2. When calculating the number of load repetitions necessary to achieve a rut depth of 20 mm, the situation after preloading was set as the zero level because the actual loading aiming at deformation of the structure only began after the preloading. The Figure shows that rutting is not linear in relation to the number of passes. Instead, plastic deformations are greater in the early stages of loading. A single wheel was used during the first 1,500 load repetitions, which explains the quite rapid development of the maximum rut in the beginning. When the test wheel was changed to a dual wheel, the development of the maximum depth almost came to a halt at first because the dual wheel mainly widened the rut formed by the single wheel.

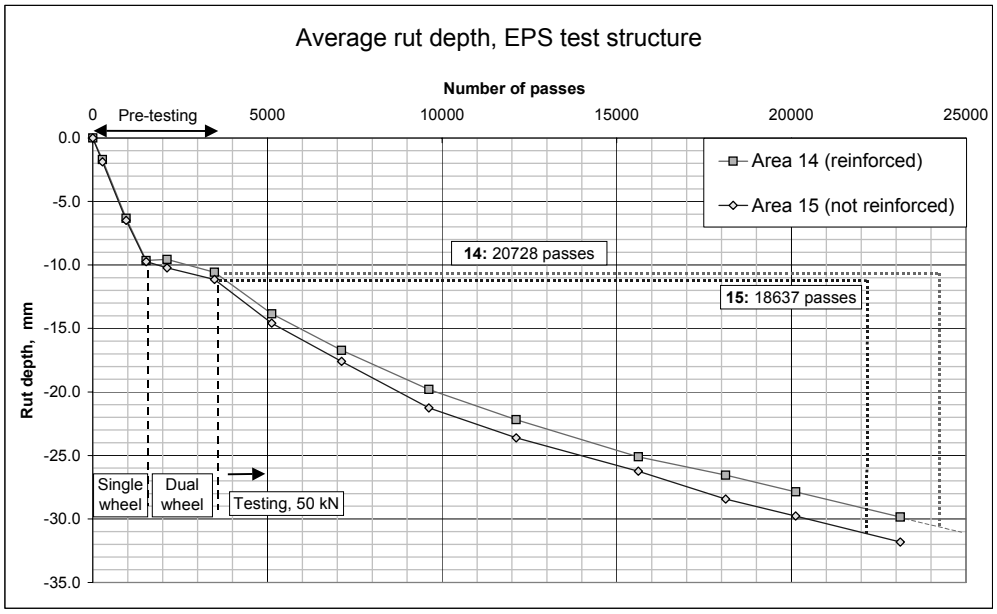

Figure 3.2. Rutting of the structure's surface on different test areas. The Figure shows the number of passes necessary to achieve a rut depth of 20 mm from the beginning of actual testing (dual wheel, wheel load 50 kN) /Elomaa 2002/.

The resilient and permanent vertical deformations in the pavements of the test structure were determined from the measurement results of the EmuCoil sensors.

Figure 3.3 shows the relative vertical deformation of the EPS layer on different wheel loads during preloading. The total number of passes was under 3,532 and the maximum depth of ruts in the surface layer was approximately 11 mm. The relative deformation measured in the EPS on 50 kN wheel load was at this stage 0.66% in the reinforced area and 0.60% in the unreinforced area.

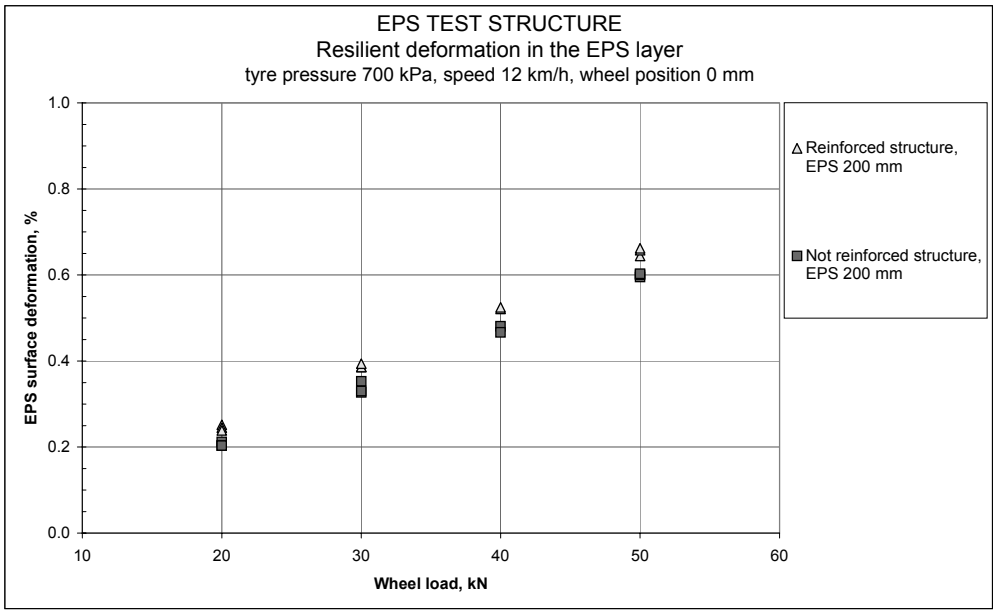

Figure 3.3. Relative deformation in the EPS on different wheel loads /Elomaa 2002/.

3.3 The effect of sloped structures

The basis for the test structure design (tests 16–20) was to construct a structure that corresponds to the structure of a low-volume road. In actual practice, the structure was designed with a multilayer programme to have such a load capacity that the structure rutted sufficiently under a reasonable number of load repetitions (approximately 15,000 passes). That is, the structure was not designed to correspond to any actual road class /Korkiala-Tanttu *et al*. 2003a/.

According to the compaction measurements, the average degrees of compaction achieved were quite good both for subbase and for the base course. However, the bearing capacities defined on the basis of the Loadman measurements were clearly below the general minimum bearing capacity for the subbase (105 kPa) and for the base course (215 kPa).

The thickness of the surface layers was also thinner than designed. The average thickness of the surface layer in the structure with no slope was 47 mm, that of the structure with a gentle slope 37 mm and that of the structure with a steep slope 41 mm. On the basis of the APAS calculations, it can be estimated that the 10 mm difference in the thickness of the surface layer increases stress in the base course by 11–29% and in the subbase by 5–11%.

The purpose of this research sub-project was to study the behaviour, bearing capacity, deforming and deterioration of various pavement structures with a slope under a Heavy Vehicle Simulator (HVS) load simulating the passing of a lorry. Test parameters of tests 16–20 are shown in Appendix 1.

The extent of permanent deformations in the structures was monitored with Emu-Coil measurements. The top coils of the upper Emu-Coil sensors were levelled after the tests and the deformation of the base course and the surface layer was calculated from the results. It was assumed that the asphalt layer did not deform. Figure 3.4 shows the proportion of deformation in each layer of the total rutting defined in this way. Changes in the water table level had a crucial effect on the results, so the comparisons were based on cases in which the water table level was identical, +15.95.

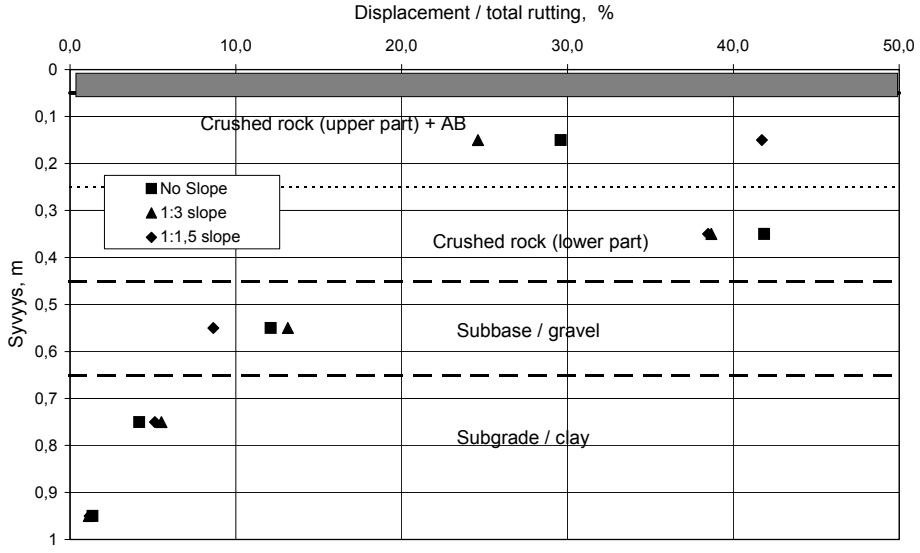

Figure 3.4. Proportion of the deformation of the total rutting in 200 mm layers, with the water table level in all the structures at +15.95 /Korkiala-Tanttu et al. *2003a/.*

The results indicate that in structures with no slope or with a gentle slope, the greatest deformations occur in the lowest part of the base course, while in the structure with a steep slope, the deformations were equally large in both parts. 63–80% of permanent deformations occur in the 400 mm thick base course and the surface layer. The share of the subbase (200 mm) of the settlements is approximately 9–13%, and that of the upper parts of the subgrade (400 mm) 4–6%.

The development of permanent deformations in the steep slope structure under different loads and passes is presented in Figure 3.5. The deformation for the upper part of the crushed rock is calculated, and the others are based on Emu-Coil measurements. In both structures with slopes the deformations concentrate more strongly in the upper part of the crushed rock the greater the load and the higher the water table level.

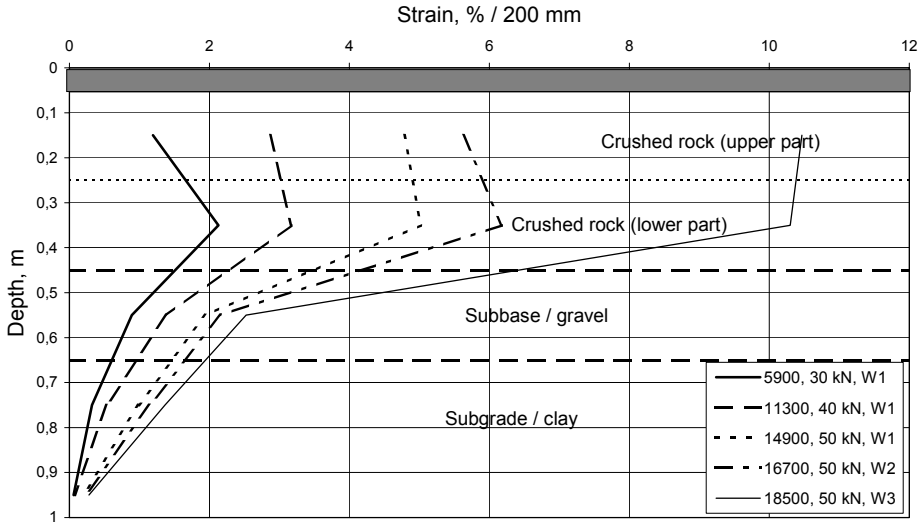

Figure 3.5. Development of deformations under different loads in the structure with 1:1.5 slope / Korkiala-Tanttu et al*. 2003a /.*

The ratios of resilient and permanent (plastic) horizontal deformations adhere to the principle that permanent deformations increase as resilient deformations increase. Figure 3.6 shows the ratio of horizontal deformations in the lowest part of the crushed rock under a load of 50 kN. Both resilient and permanent deformations were measured with lateral displacement gauges in the slopes.

Figure 3.6 shows a clear increase in permanent deformations per pass once a certain threshold value in resilient deformations is exceeded. This threshold value for crushed rock and gravel is approximately 100 μm. The extent of resilient deformations depends on the stress state prevalent in the structure at the time. The increase in permanent deformations is also significantly influenced by changes in water content and the steepness of the slope.

The great differences in resilient horizontal deformations, while the steepness of the slope and the water content remained the same, are due to the way the structure was loaded. The structure was loaded in cycles of 600 passes so that the loading wheel was first positioned on the left side of the rut, approximately 300 mm from the centre, then in the centre and finally 300 mm to the right of the rut. The greatest displacements were naturally observed in the load position where the wheel was nearest to the slope, and the smallest when the load was the farthest from the slope.

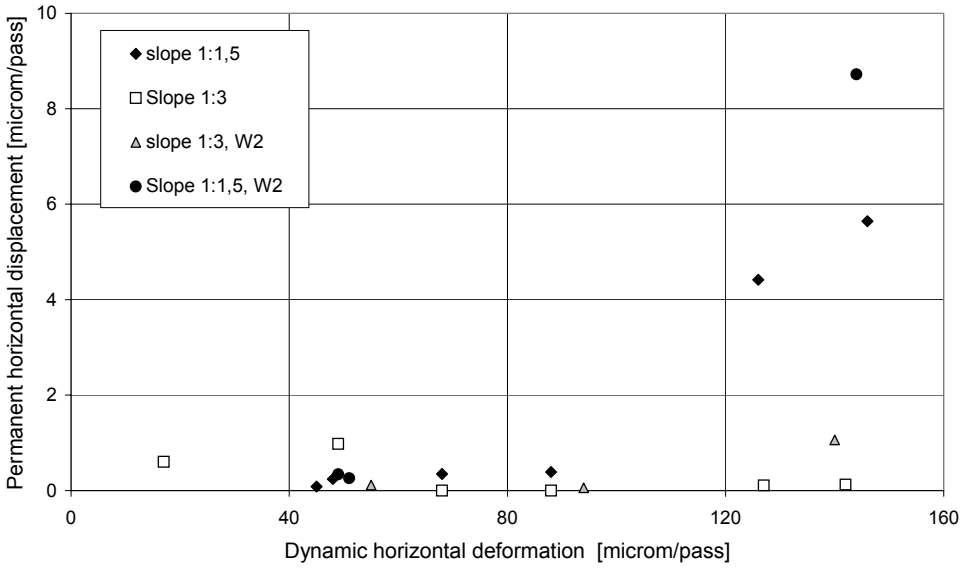

Figure 3.6. Figure 3.6. Ratios of horizontal deformations in the lowest part of crushed rock under a load of 50 kN /Korkiala-Tanttu et al. *2003a/.*

When the transient stress state of the structure (earth pressure σ_{zmax}) and resilient deformation ε_{zmax} (Emu-Coil) are known, the corresponding dynamic resilient moduli can be determined. Earth pressure was monitored in both the gravel and clay layers. The average values for the moduli are given in Table 3.1.

Table 3.1. Average resilient moduli in clay and gravel layers for different structures /Korkiala-Tanttu et al. *2003a/.*

Structure	Resilient modulus, gravel, MPa	Resilient modulus, clay, MPa
laboratory result	80	7
no slope	62	17
1:3	46	16
1:1.5	76	15

A structural deformation design method developed in the Low-volume road project represents the width of the road and the steepness of the slope with the GEOM factor. The GEOM factor was determined in the HVS test on the basis of the development of rut depth measured by a profilometer.

In order to determine the GEOM factor, there was data on the development of rut depth inflicted on the structure on different structures, different distances from the edge of the slope and different loads. As for the road width that affects the factor, it was decided on the basis of the results that loading 450 mm from the edge corresponded to a road width of 5.5 m, loading at 750 mm to 6.5 m and loading at 1050 mm to 7.5 m. The solution was arrived at on the basis of average rut positions measured on roads. That is, the GEOM factor cannot be directly applied for roads with wider pavements.

Because of the limitations caused by the increase in water content on the structure with no slope after 9,500 load repetitions, it was decided to use the development of rut depth for 500 to 9,500 passes as the basic data for all the structures (load 30/40 kN) and, for sloped structures, the development of rut depth that occurred at 11,300 to 14,900 passes (load 50 kN). A suitable fitted curve was sought on the basis of these rutting speeds. In the last phase of determining the GEOM factor, the value of the rutting speed for 6.5 m road width and 1:3 slope was set as a reference value. The value of this rutting speed was defined as 1 and other figures were converted to correspond to the reference value. Figure 3.7 presents the value of the GEOM factor developed in a graphic format.

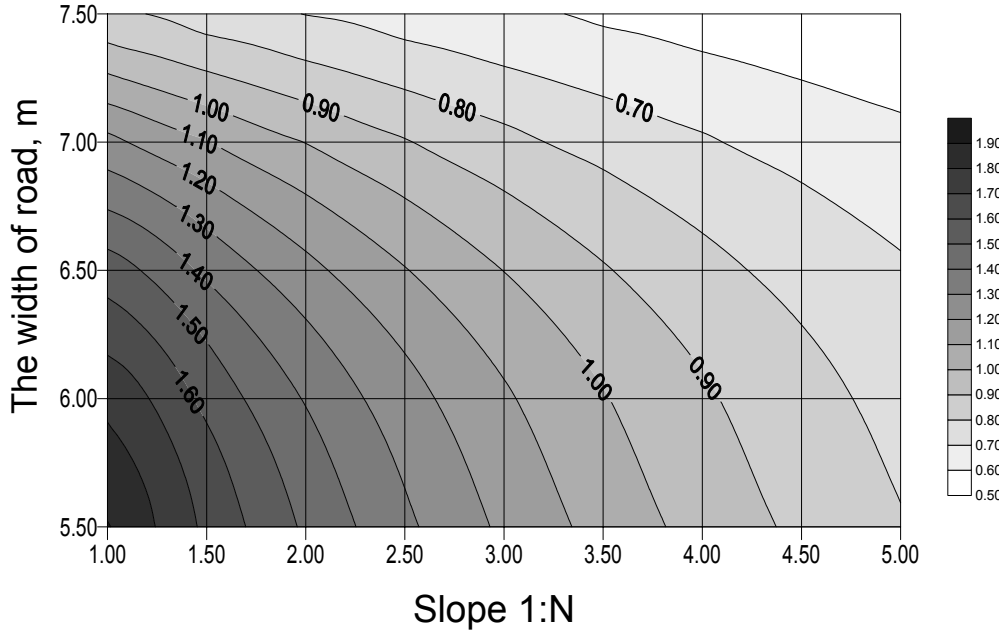

Figure 3.7. GEOM factor as a function of slope steepness and road width /Korkiala-Tanttu et al. *2003a/.*

3.4 The effect of spring and overload

The structures of tests 21–23 were pavements to be tested for low-volume roads. They belonged to a study *"Effect of spring and overload on the rutting of a low-volume road",* which complemented the Low-volume road structures project /Korkiala-Tanttu *et al*. 2003b/.

The aim of the study was to acquire basic information on the behaviour of road structures with low bearing capacity. The study also aimed at discovering whether the fourth power rule applies, as well as the effect of spring on low-volume roads under a Heavy Vehicle Simulator (HVS) load imitating the passing of a lorry. Test parameters are shown in Appendix 1.

The starting point for designing the test structures was that the structure would be designed to correspond to the structure of low-volume roads. The corresponding measurable requirement values have been laid down by the Finnish Road Administration Finnra TYLT. However, these values were not aimed at in every respect, especially as regards bearing capacity.

Because the construction site is small and the basin narrow, it was difficult to reach the same kind of quality during construction as for larger sites. This applies to the thickness and quality of the surface layer in particular. The thickness of the surface layer was calculated from the levelling results and determined by eddy-current measurements. According to the measurement results, the surface layer of the middle structure (structure 22) was clearly the thickest (60.8 mm). The average thickness of structure 23 was 59 mm and that of structure 21 50 mm. The differences were large and probably due to the fact that it was difficult to correctly adjust the asphalt paver on such a short structure. The falling weight deflectometer measurements also showed that the bearing capacity of structure 21 was the lowest and the bearing capacity of the middle structure (22) was the highest.

The bearing capacity of the structure was also measured after the testing ended. The bearing capacities calculated at that time varied between 142 and 237 kPa. These measurements showed that the middle structure (structure 22) had the highest bearing capacity (on average 217 kPa) and structure 23 was the weakest (on average 196 kPa). Presumably the structure compacted during the testing, because according to the FWD measurements, the bearing capacities increased in the testing.

The rut development of the test structures has already been presented in Chapter 2. Because the thickness of the surface layer was not identical in all the structures, the deformations of the thicker structures (22 and 23) were converted layer by layer in relation to the thickness to correspond to deformations in the structure with the target thickness (50 mm). The overall estimate was that the rut depth of structures over 60 mm thick with the ground water at the higher level was increased by 14.5%. If the ground water level was lower, but the thickness of the surface layer was over 60 mm, rut depth was increased by 10%. In addition, the rutting of a structure with a load of 50 kN and ground water level at -1.0 m was estimated by calculation. This estimate was based on the rutting speed with a 50 kN load obtained at the beginning of the test.

The rut depth estimated by calculation for a 50 kN load with the lower ground water level is 8.8 mm when the number of passes is 70,000. After making the correction for the thickness of the surface layer, the estimated rut depth for 70 kN load is 24.4 mm. Correspondingly, with the higher ground water level, the rut depths are 20 mm and 60 mm. That is, rut depth is 2.8 to 3 times higher when the load is increased from 50 kN to 70 kN. Raising the ground water level by 0.5 metres increases rutting 2.2 to 2.45 times. If both load and ground water level increase, the rutting increases 6.8 times. These ratios are only approximate and naturally depend on the structure, its state of compaction etc.

Cross directional rutting of the pavements was monitored with settlement profile measurements. Figure 3.8 shows the rutting of the pavements in the most rutted structure, structure 21. The Figure shows that rutting in all pavements seems to be mostly compaction and there is no significant shearing action. When estimating the distribution of the rutting area in the pavements from the Figure, it can be seen that deeper down in the structure, the rutting spreads over a very wide area.

At a depth of 0.5 metres, on top of the sand layer, the width of the rutted area was approximately 2.5 metres, while the width of the entire loading area on top of the surface layer was 1.15 metres. This means that the load spreads in the sand layer according to the ratio 1:1.35. The width of the rutted area reveals over how wide an area stresses were distributed in the layer. A commonly used assumption in geotechnical engineering is that the stresses are distributed in a ratio 2:1 to the soil layers beneath. Thus, in road structures the stresses are clearly distributed over a wider area than the above assumption would predict, causing displacements to also decrease. In other layers, the distribution is even wider in relation to the thickness of the layers above, the ratios being approximately 1:4.5 for the bottom of the surface layer / top of base course, 1:2.7 for the top part of base course (100 mm), 1:1.7 for the bottom part of base course / top of subbase and 1:1.35 for the bottom of subbase / top of subgrade.

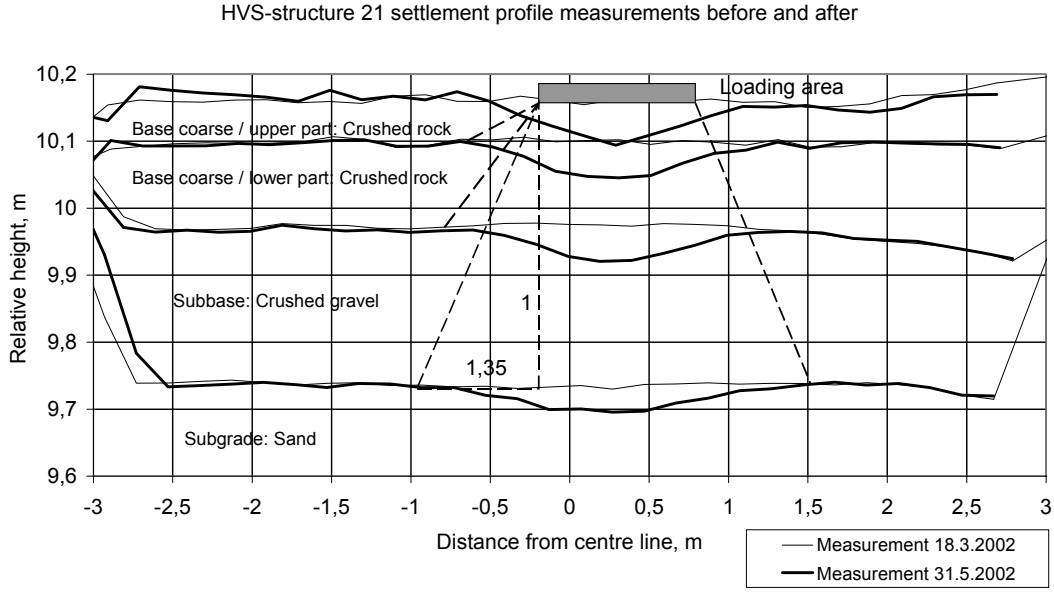

Figure 3.8. Rutting of pavements in structure 21 according to settlement profile measurements /Korkiala-Tanttu et al. *2003b/.*

Distress in the structures was also monitored during the testing. The distress was photographed and recorded on a map. No large cracks were discovered in the structures, but some narrow longitudinal cracks were observed. Table 3.2 presents the formation of cracks in different structures.

Table 3.2. Formation of cracks in the structures / Korkiala-Tanttu et al. *2003b/.*

Structure	N number of passes	Number of cracks	Cracks (length, cm)
21	27000	0	0
21	32100	3	60
21	52500	3	110
21	70060	4	140
23	40020	0	0
23	70000	1	100

Permanent deformations in the structure were monitored with Emu-Coil, settlement profile and eddy-current measurements. Settlement profile and eddy-current measurements were only conducted at the beginning and end of the whole testing. The rutting of the surface layers' surface was monitored with profilometer measurements. Figure 3.9 presents the proportion of displacement in different layers in the total rutting combined from different measurements.

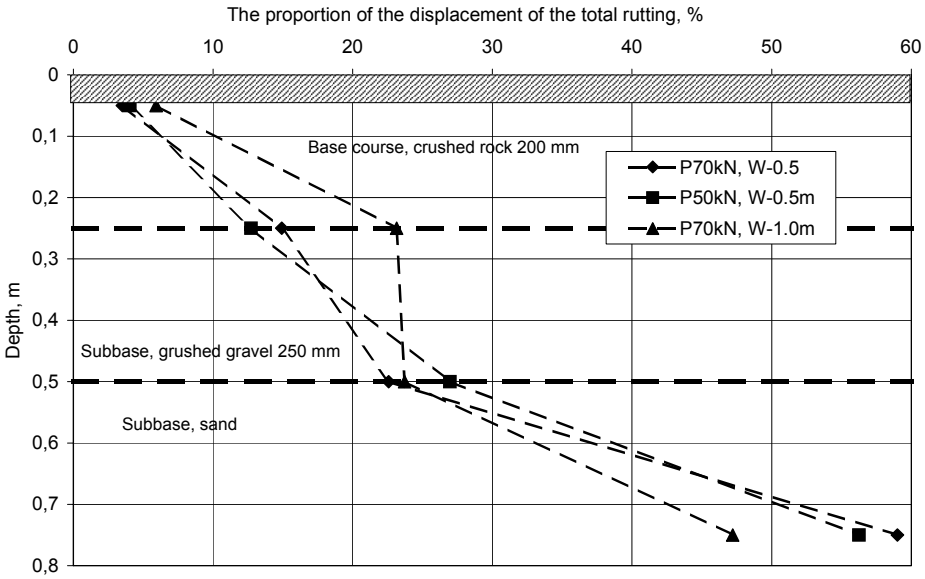

Figure 3.9. Proportion of deformations in different layers of the total rutting / Korkiala-Tanttu et al*. 2003b /.*

The graphs in Figure 3.9 follow the same pattern surprisingly well. The largest share of rutting (47–59%) for each load occurs in the subgrade. When the ground water was lower, a greater proportion of displacements occurs higher up in the base course. When the ground water level is raised, a proportionally larger share of settlement occurs lower down in the gravel and sand. The proportion of the surface layer of the rutting was 3.5–6%, that of the crushed rock in the base course 15–23% and the crushed gravel in the subbase 23–27%.

The fourth power rule is used for estimating the damage to the surface layer of a road. The rule is empirical and was developed on the basis of AASHO road tests conducted in the United States in the 1950s. The tests monitored different road structures and their distress over a period of many years. The monitored sites can mostly be classified as high-volume roads and their bound layers were thick, that is, they were not low-volume roads. The rule says that the ratio of distress or the number of load repetitions increases in relation to loads according to Formula 3.1, when the tyre pressure used in the loading remains the same. When estimating the rutting of roads with an asphalt surface layer, the index n value used, on the basis of AASHO road tests, is usually 4.

$$E = \left(\frac{P_x}{P_{st}} \right)^n \qquad (3.1)$$

in which

E		equivalent coefficient of the load
P_x		the axle load studied
n		index
P_{st}		standard axle load

Figure 3.10 presents the ratio of the number of passes for different rut depths determined for 50 and 70 kN loads when the ground water level was at -0.5 m from the top of the surface layer. Distress is only described by rut depth. The share of compaction (the first 900 passes) has been excluded from calculating the ratio of the number of passes. Furthermore, the calculations take into account the variation in the thickness of the surface layer in different structures. The rutting curve for 50 kN load is linearly extrapolated for rut depths of over 18 mm (Figure 3.10 calculated values).

According to Formula 1, the development of distress should be independent of rut depth. The value for the equivalent coefficient for the standard load of 50 kN and the axle load studied, 70 kN, is approximately 3.8 (the horizontal line in Figure 3.10), when the value used for the index n is 4. However, the ratios of the number of passes (N/N_s) calculated from rut depths are clearly larger, in the order of 6 to 18. The index n in Formula 1 varies between 5.5 and 16. Thus, the results reveal that the fourth power rule is not applicable for low-volume roads. The HVS tests in the low-volume road project indicated the same.

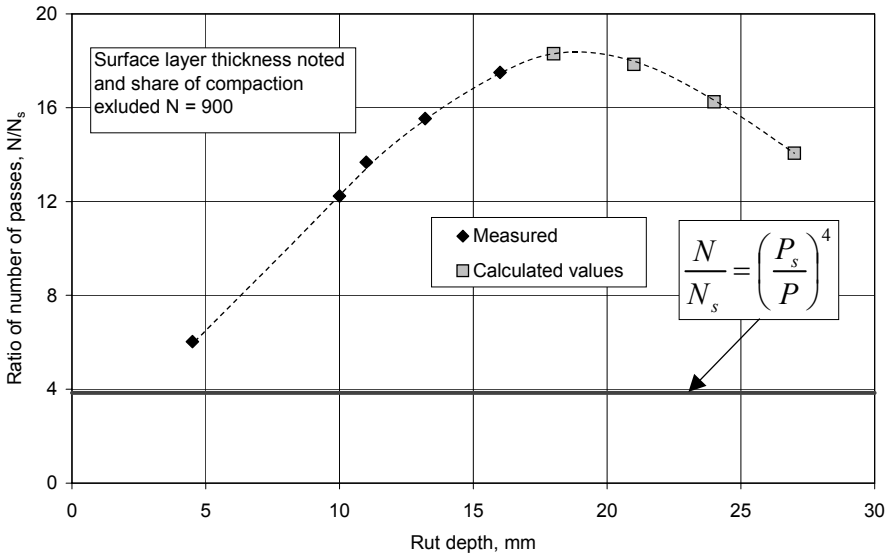

Figure 3.10. Ratio of number of passes with different rut depths / Korkiala-Tanttu et al. *2003b /.*

The fourth power rule is an empirical relationship that is established on the basis of a statistical analysis, and the only factor affecting distress that it takes into account is load. Especially in cases in which behaviour is governed by permanent deformations, quite non-linear in nature, it is not surprising that the fourth power rule does not work. Thus, such a simplified rule cannot be used for modelling the road deformations on low-volume roads.

The relation of resilient and permanent vertical deformations in different materials was compared by Emu-Coil measurements. Resilient deformation is the total deformation caused by one pass, which includes both permanent and dynamic deformation. The share of permanent deformation of the resilient total deformation is, however, so small as to be trivial. Figure 3.11 presents these relations of deformations for subgrade sand. The results clearly show a threshold value for resilient deformations / stress state, after which permanent deformations clearly increase faster. Similar behaviour was observed in other materials, although the results varied more. The phenomenon is familiar from theories of soil behaviour, in which the limit is described, for instance, as exceeding the (soil elastic) limit state. The limit deformation presented in Figure 3.11 commonly depends not only on the material, but also its state (moisture, density and stress state).

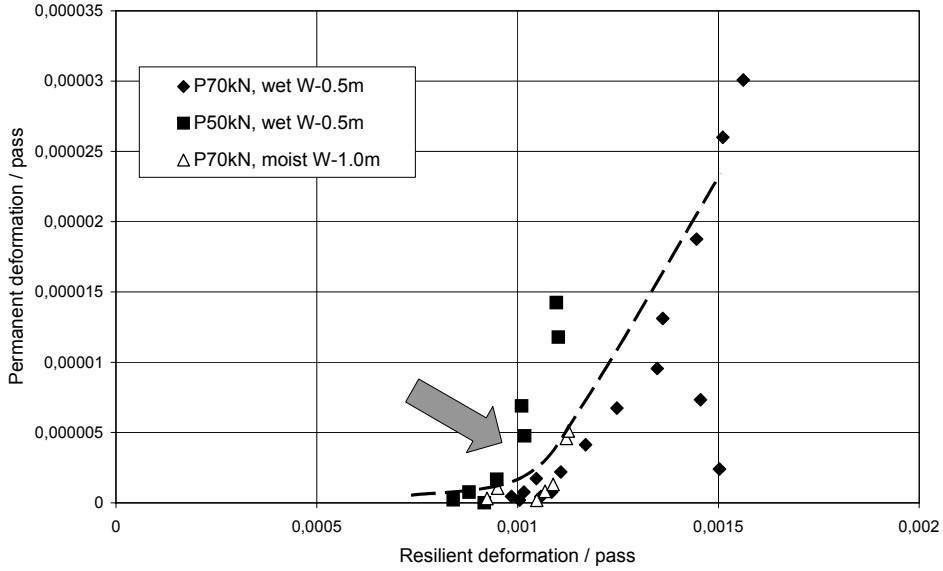

Figure 3.11. Relation of dynamic and permanent deformations in subgrade sand /Korkiala-Tanttu et al*. 2003b /.*

3.5 Reinforcement of the edge of a steep-sloped pavement

The main aim of the research was to study what effect the reinforcement grid used in the rehabilitation of rutted structures has on decelerating rutting in structures with low bearing capacity edges. The second aim was to find out whether different reinforcement grids differed in decelerating rutting.

Levelling during rehabilitation monitored the thickness of the rut levellings and asphalt layers. According to the levelling, the total thickness of the asphalt layers on the loaded area ± 300 mm from the centreline were:

- structure 24–25: 139 mm
- structure 26–27: 175 mm
- structure 28–29: 188 mm

Because of these differences in the thickness of the bound layers and in the steepness of the sideslope in the Low-volume road tests, the structure pairs were in different states before the testing began.

When dismantling the structures, it was discovered that there were great differences in the adhesion between the old and new surface layer. Some structures, such as the fibreglass mesh glued with bitumen emulsion, adhered to the surface layer uniformly, while in structure 24–25, the new surface layer and the steel grid embedded in it had come completely apart. The surface layers had also come unstuck in the corresponding reference structure.

The displacements in this test were significantly smaller than in the previous test. Figure 3.12 presents the proportion of different layers in the total rutting.

The data for the upper part of the base course could not be determined sufficiently reliably due to inadequate measurement results. However, subsequent measurements of the structures clearly indicated that the majority of deformations had occurred in the base course. According to the Emu-Coil measurements, the lower part of the base course accounted for 16–22%, the gravel 13–17%, the upper part of the clay 7–13% and slightly lower parts of the clay for 1–14% of the total rutting. It is probable that by far the largest deformations in this test occurred in the upper part of the base course. Some of the remaining deformations occurred lower in the clay. The distribution of deformations differs from that of the first phase, in which the upper and lower parts of the base course deformed more or less equally.

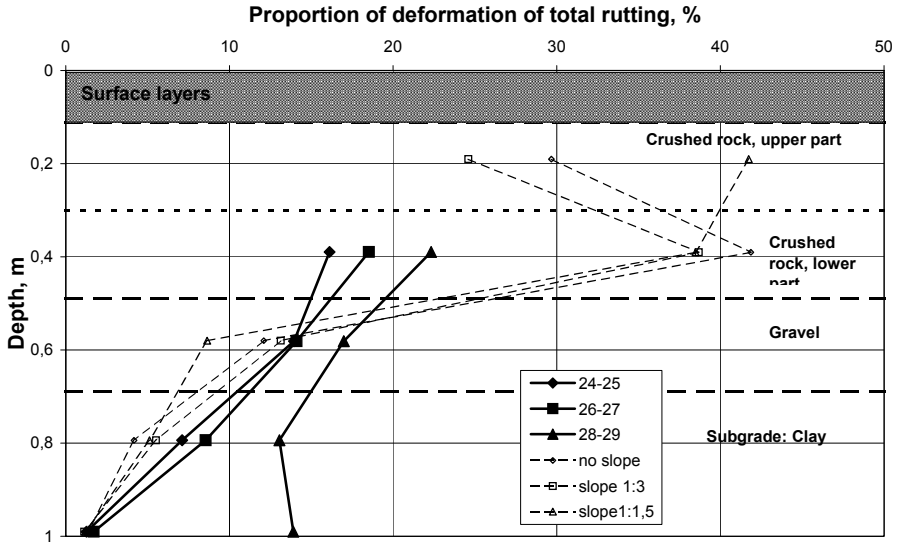

Figure 3.12. Proportion of vertical displacement of pavement in the total rutting of the surface.

The level of deformations in unbound layers remained low in rehabilitated structures, as Figure 3.13 indicates. It is not possible to determine the threshold value for plastic performance (shakedown value) for different loads or moisture contents on the basis of the results of this test alone. Figure 3.13 also shows the deformations of the corresponding structures in the first test phase. The threshold value can be roughly estimated from the combined results of these two tests. No great differences were observed in the ratio of deformations between the different structures. The Figure does not show the ratio of deformations in the preloading stage. Instead, it only presents the stage of 'decelerating' performance.

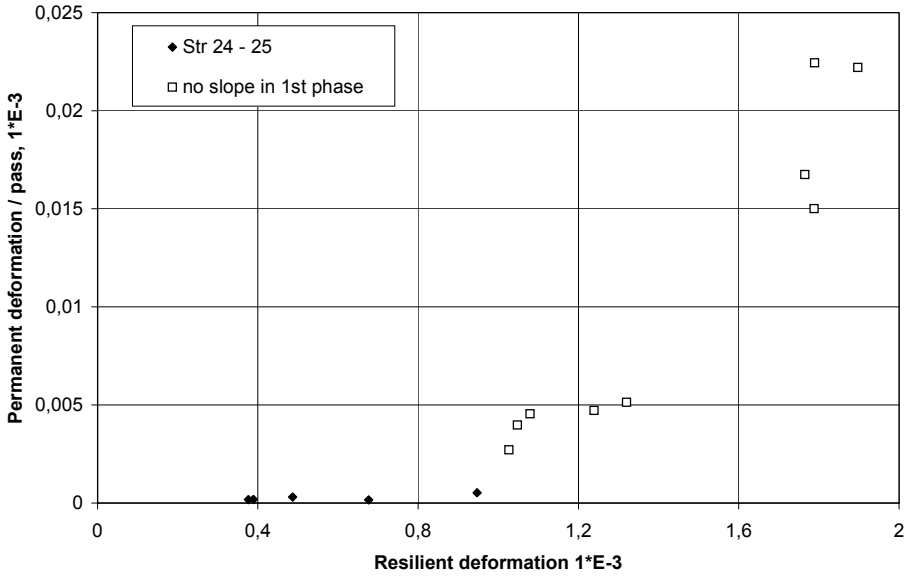

Figure 3.13. Structure 24–25. The ratios of permanent and transient vertical displacement in the crushed rock layer in this and the Low-volume roads study.

The earth pressure values for unbound layers showed a clear decrease thanks to the rehabilitation of the structures. Earth pressure was only monitored between different structure pairs because the location of the earth pressure cells varied within the pairs of structures, some being in the reinforced and some in unreinforced areas. In the gravel layer, the decrease was approximately 42% in structures 24–25, and in structures 28–29 approximately 58%. Deeper down in the subgrade clay the difference was also approximately 28% in structures 24–25 and, on average, 48% in structures 28–29. The values in structures 26–27 fall between these values.

The clearly smaller deformations in the rehabilitated structures are significant. Although the gravel layer's earth pressure in the rehabilitated structures decreases 42–58%, the deformations decrease even more in proportion, 65–82%. The decrease in the earth pressure in the clay layer is slightly less, 38–48%, and the corresponding decrease in deformations 47–74%. It is easy to see from this ratio that the relation between deformations and stress state is non-linear (Figure 3.12)

Load has very little effect on the tensile strain observed in the steel grid. According to measurements, the additional tensile strain in the steel grid caused by load is typically only 10% of its permanent tensile strain. At this stage, the results seem to indicate that the thickness of the bars in the steel grid has no effect on rutting speed. In other words, the capacity of the steel grid with thinner bars is great enough to receive the mobilised stress without major deformations. Furthermore, it seems that the worse the condition of the original structure the better the reinforced structure performs.

Falling weight deflectometer measurements were carried out before and after testing. The results are presented in Table 3.3. The bearing capacity values for the fibreglass reinforcement are clearly the smallest, while the index values were the highest. The differences between the bearing capacities of reinforced and unreinforced structures were small (1–22%). The differences in the values of the SCI indices, describing the shape of the deflection bowl, were slightly higher (0–25%), when comparing only the steel grids. Comparing the structure pairs 24–25 and 28–29, the greater differences in bearing capacity and SCI indices in structure pair 28–29 indicate better performance of the reinforcement.

Other studies have also concluded that falling weight deflectometer measurements do not reveal great differences between reinforced and unreinforced structures. Therefore, the better performance of a reinforced structure cannot be reliably measured with a falling weight deflectometer. It is possible that the SCI index could give a slightly more reliable value, but it would also be only an estimate.

Table 3.3. Surface bearing capacity values and SCI indices calculated from falling weight deflectometer measurements (before/after testing).

Test	FWD surface bearing capacity	SCI300 (μm)	SCI450 (μm)
Str 24 (reference)	128 / 98	411 / 564	542 / 772
Str 25 (steel grid 6 mm)	136 / 105	397 / 566	504 / 747
Str 26 (steel grid 8 mm)	142 / 102	371 / 585	472 / 775
Str 27 (Polyfelt PGM-G100/100)	125 / 114	467 / 511	592 / 667
Str 28 (steel grid 6 mm)	138 / 104	394 / 578	499 / 764
Str 29 (reference)	120 / 85	446 / 716	572 / 960

The service life of structures – here the number of passes – can be estimated with the help of different extrapolations. The aim was to discover the structure's service life corresponding to a rut depth of 15 mm. The extrapolations were conducted on the basis of the last loading stage, in which the wheel load was 50 kN and the water table level W3, that is, the ground water reached the middle of the base course. The greatest uncertainties in the estimation are related to structures with shallow (under 5 mm) ruts.

The simplest way to carry out the extrapolation is to continue rutting at the same speed (linear extrapolation). In the estimate, the rutting speed is determined on the basis of the difference of the last two observations. The calculation results are given in Table 3.4.

Linear extrapolation does not take into account the deceleration of rutting as the number of passes increases, which is why a non-linear extrapolation based on a power function was also carried out. The extrapolations were carried out with Excel spreadsheet software by fitting the power function to all the observations (3 to 4 observations) of the last loading stage (load 50 kN, water table level W3) by searching for the smallest value of the sum of squares of the difference of the results. The results of the calculations are given in Table 3.4.

Table 3.4. Number of passes resulting in a rut depth of 15 mm for different extrapolation functions.

Test	A. Linear fitting	B. Power function fitting
Str 24 (reference)	45,350	46,300 ($u = 0.00161*N^{0.895}-9.17$)
Str 25 (steel grid 6 mm)	64,400	66,800 ($u = 0.00081*N^{0.900}-2.81$)
Str 26 (steel grid 8 mm)	89,100	87,300 ($u = 0.00147*N^{0.825}-2.51$)
Str 27 (Polyfelt PGM-G100/100)	102,000	87,700 ($u = 0.0831*N^{0.505}-10.94$)
Str 28 (steel grid 6 mm)	146,200	194,500 ($u = 0.0280*N^{0.538}-4.80$)
Str 29 (reference)	61,750	66,800 ($u = 0.2406*N^{0.437}-15.67$)

When comparing unreinforced reference structures and reinforced structures, it can be concluded that the rutting speed of a reinforced structure is slower than that of an unreinforced structure. According to this comparison, the rutting of reinforced structures reduces by 40–150%, which corresponds to an increase of 40–190% in the structure's service life. The reinforcements were especially effective in the structure pair 28–29, which was in the poorest condition at the outset, but the shape of which was not changed during the tests. The different performance of corresponding structures is probably also due to how well the asphalt layers adhere to each other. No major differences were perceived in the rutting speeds of the different reinforcements.

4 DISCUSSION

The construction of the test structures inside basins was done very carefully to get as even constructions as possible. The quality of the construction was monitored with levelling, density and bearing (FWD, Loadman) tests. Despite this, the quality measurements showed that there was a large scattering in some properties. The biggest problem was the thickness of the asphalt layer and hence the bearing capacity of the structures. The average thickness of the asphalt layer in the Low-volume test series varied from 37–47 mm. The calculations by a multilayer programme showed that a 10 mm decrease in asphalt thickness increases stresses by about 11–29% in the base layer and 5–11% in the subbase. This problem was common to all test structures.

There are two opposing views regarding where the permanent deformations occur. One argument is that the most significant part of the permanent deformations occurs in the base course. According to the other argument, it is the subgrade that deforms. The HVS test results show that both arguments are correct and depend on the structure. In the Low-volume test it was the base course that deformed (Figure 3.4) and in the Spring–Overload test it was the subgrade that deformed the most (Figure 3.9). So, from the surface of a moderately rutted road it is impossible to know where in the structure rutting really will happen and how deep the ruts will be. The only possible method is to calculate permanent deformations in different pavement layers. The calculation of permanent deformations is not a simple task. There are only a few material models for the permanent deformations, which takes into account the capacity, the number of the passes and the stress state. One of the best available models is presented by Huurman /Huurman 1997/. VTT modelled the Low-volume test structures with an element program called Flac. The calculation was made using material properties, which had been determined in the laboratory. Even with simple material models a relatively good correlation between calculations and the real behaviour of the test structure was achieved.

Rehabilitation also affects the accumulation of permanent deformations of the structure considerably. The total rutting of the Steep slope test was much smaller than the rutting of the Low-volume test (Figure 3.13) although the number of passes was doubled in the Steep slope test.

The effect of the water content and magnitude of the load was studied in the Spring–Overload test (Figure 2.14). There were two different water levels (1.0 m and 0.5 m depth from the asphalt surface) and two different loads (50 kN and 70 kN), which were compared with each other. While there were only three test structures, the reference structure with a 50 kN load and a -1.0 m water level was assessed from the other test results. Figure 2.14 clearly shows how much the change in water content or load affects the rutting. The basic situation when the wheel load was 50 kN and the water level was deep (-1.0 m) was extrapolated from the preloadings. When the water level rose half a metre the rut depth increased 2.2–2.5 times. If the wheel load increased to 70 kN the depth of rut increased 2.8–3 times. If both water level and load level increased the depth of rut increased 6 times more than in the basic situation. The change in water content of the partly saturated base course and subbase was only 0.3–0.4 percentage units, yet its effect was drastic.

It is well known that the deformation behaviour of granular materials is highly non-linear. Many studies have shown that there is some limit value of the transient load after which the permanent deformations will grow quickly. This limit value is usually called the 'shakedown' limit in highway engineering. This phenomenon corresponds to the yielding in geotechnics. The 'shakedown' limit can be clearly seen when both resilient and permanent deformations are compared with each other (Figures 3.6, 3.11 and 3.13). The value of the 'shakedown' limit depends on many things, the most important of which are the material, water content, stress state and density. In the Steep slope test the 'shakedown' limit was not exceeded so the permanent deformations were quite moderate.

All the test results both in laboratory and in field conditions showed that rutting (the depth of the rut) can be significantly reduced by using steel grids in bitumen bound layers or unbound base. On average this reduction lies between 40 and 60%. There are some tests that indicate even 60% reduction of rut depths. The effect of the steel grid is small in structures with thick bound layers or otherwise good bearing capacity. The reduction of the rut depth by 40–60% means that the service life of a reinforced pavement is about 50–100% longer than the service life of an unreinforced pavement in respect to rutting. The reinforced structures had been reinforced mainly with steel grids.

The efficiency of the reinforcement depends on the conditions where it is used. The reinforcement works best in the cases where the bearing capacity of the pavement is low. If the bearing capacity of the pavement is high, reinforcement does not reduce the rutting speed much (Figure 4.1). Figure 4.1 contains also test results of the previous HVS Frost test /Kangas *et al.* 2000/. In the tests the surface moduli – which indicates bearing capacity – have been measured with falling weight deflectometer or with Benkelmann beam in the Frost test.

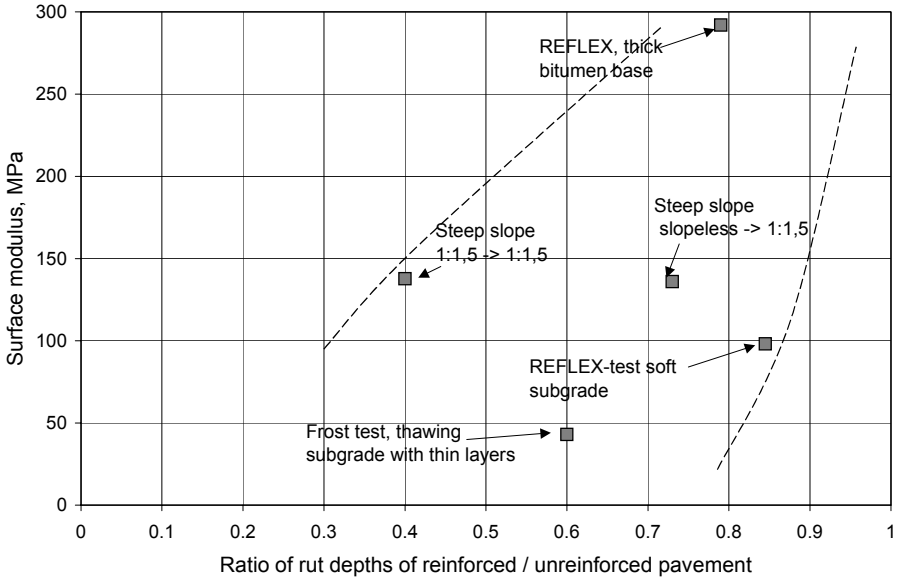

Figure 4.1. Ratio of the rut depths of reinforced and unreinforced pavements in respect to the surface modulus in different HVS tests. The reinforcement works more efficiently when the surface modulus is low.

5 CONCUSIONS

5.1 Tests 11–13

The main objective of REFLEX (”*Reinforcement of Flexible Road Structures with Steel Fabrics to Prolong Service Life*”) was to develop new technology for road construction and rehabilitation. The idea is to use steel fabric reinforcement in asphalt roads in order to make road structures more cost effective by improving the lifetime of new roads and by developing an optimal rehabilitation method for existing roads.

The accelerated tests could be done in a reasonable time and all the test pavements deteriorated. The deterioration mode was more rutting than cracking.

In all three REFLEX tests (two in Sweden and one in Finland) steel reinforced pavements performed better than reference pavements, when the deterioration mode was rutting. When the deterioration mode was cracking there was no clear difference between steel reinforced and unreinforced pavements.

In the Finnish bearing capacity tests (Reflex03 alias tests 11 and 12), where steel grid was installed in unbound base course, the reinforced sections tolerated 50–100% (depending on rutting level) more load repetitions than the (unreinforced) reference structure at the same rut level.

According to earlier tests carried out in Finland, a reinforced section constructed on thawing frost susceptible subgrade tolerated 100–250% (depending on the rutting level) more load repetitions than the (unreinforced) reference structure at the same rut level. In the bearing capacity test, where steel grid was installed in unbound base course, steel grid made the unbound base course stiffer and it tolerated rutting in the base course. The pavement response measurements explained mainly the better behaviour of steel reinforced pavements in the bearing capacity test, where steel grid was installed in the unbound base course.

The stress due to wheel load in subgrade, for example, was 20% greater in the unreinforced structure compared to that of the steel reinforced structure. During the test, the stress in the subgrade in the unreinforced structure increased considerably. The increase in the stress in the steel reinforced structure was much less. Stress in the steel grid bar also increased during the test. That meant the steel grid took horizontal forces in the unbound base course.

After the excavations the steel grid could be seen to have the same form as the interface between the base course and subgrade. This meant that the steel grid had behaved as an integral part of the base course and no base course material had gone through the steel net.

5.2 Tests 14 and 15

Falling weight deflectometer measurements showed that the structure reinforced with a steel grid did not have a better bearing capacity than the unreinforced structure in the EPS test structures (tests 14 and 15). The deflection bowls measured before test loading were also almost identical on both structures. However, the deflection bowls determined after the testing gave a greater modulus for the lower part of the crushed rock in the reinforced structure than in the unreinforced structure.

The rutting of the structure reinforced with a steel grid and the unreinforced structure were also similar. In these circumstances, the steel grid did not have a significant effect on the rutting as the rutting seemed to occur mainly above the grid. It would perhaps have been more advisable to place the steel grid in the middle of the crushed rock layer, enabling the grid to function as a shear reinforcement.

The rutting was mainly due to deformation in the crushed rock above the EPS layer. The sand below the EPS also rutted significantly, whereas the permanent deformation of the EPS on 20,000 load repetitions was minimal or non-existent on the vertical stress state measured, which was 75 kPa.

According to the measurements, the vertical stress and resilient deformations increased linearly in relation to the load, that is, the structure was elastic. According to the measured vertical stress and resilient deformation, the elastic modulus of the EPS layer was approximately 9.4 MPa. Back calculations gave the EPS's modulus as 10.5 MPa.

5.3 Tests 16–20

In the tests of the sloped structures (test 16–20) a great deal of measurement data was generated in different phases of the tests. The data gathered has only been analysed with regard to the aims of the study under consideration. The results will be analysed further in the future. Further research will look more deeply into the ways permanent deformations are created and the effect changes in the water content have on them.

It was possible to design the test structure in advance quite well. Although the test structure was carefully constructed, there were significant variations in the thickness of the surface layer, and the bearing capacities and densities of the layers. Preloading the structures before testing adjusted these differences slightly.

Most of the deformation in the test structures occurred in the lowest part of the base course, 240–440 mm from the surface of the road. 63–80% of the total rutting occurred in the uppermost 400 mm of the unbound layers. The share of the gravel layer deeper down was 9–13%. In the structure with no slope, the deformation maximum was located deeper (250–450 mm) than in structures with a slope – 1:3 slope in particular – in which the maximum was located the highest (50–250 mm). The speed of the rutting decreased in each load step as the number of load repetitions increased.

Changes in the structure's water content had a significant effect on permanent deformations. Permanent deformations also began to increase significantly after exceeding a threshold value for stress (dynamic deformation) that depends on the material and its state of compaction. This phenomenon was observed both in laboratory tests and the test structures. It was particularly clear for horizontal displacements. The threshold value for resilient horizontal deformation for both gravel and crushed rock was approximately 100 μm.

The location of the failure surface in different structures can be deduced on the basis of the results of the deformation measurements. The structure with a steep slope was very near failure and the deformations generated were great. The greatest horizontal displacements in the slope were located in the gravel layer, which suggests that the whole slope moved horizontally to a significant extent and that the failure surface was located deeper in the gravel layer. The greatest horizontal displacements in the structure with a gentle slope occurred in the upper parts of the slope. Most of the displacements, both horizontally and vertically, occurred in the upper parts of the structure, so the failure surface was also mainly located in the crushed rock layer. In structures with no slope, the failure surface ran through the lowest part of the crushed rock and rose higher immediately outside the loading area.

The resilient moduli back calculated for the gravel layer from the measurements were lower than those determined in laboratory tests, and the back-calculated moduli for the clay layer were higher. Correspondingly, it was observed that according to various measurements, less stresses are concentrated in the gravel layer and more in the upper part of the clay layer than was anticipated on the basis of the modelling. On the basis of studying the modelling, it can be said that the deformations and stresses appearing in the test structures during loading can be estimated reasonably well with quite rough initial values and models.

Apart from the settlement profile measurements, the results of the deformation measurements were reliable. Deformations in the structure with a gentle slope were not much greater compared to other structures even though its surface layer was, on average, the thinnest.

Rut depth, slope steepness and load distances from the edge were used to deduce the equation for the GEOM factor representing the shape of a road cross-section, which can be used for designing improved road structures. This factor allows the estimation of the impact of the cross-section on rutting speed.

5.4 Tests 21–23

In the tests of the spring and overload effects (test 21–23), a great deal of measurement data was also generated in different phases of the tests. For the time being, the data has only been analysed with regard to the aims of the study under consideration and the results will be analysed further in the future. Further research will look more deeply into the ways permanent deformations are created and the effect changes in water content have on them.

The deformations in the structures were compaction in nature. No significant generation of ridges occurred next to the ruts, and the bearing capacities of the structures increased during the tests. Only very little distress (cracks) was observed in the structures towards the end of testing. Rut depths increased 2.8–3 times when the axle load increased from 50 kN to 70 kN. Correspondingly, rut depths increased 2.2–2.5 times when the ground water level rose 500 mm. The width of the rutted area also depends on rut depth. When the ruts are deepest, the rutted area is widest. In practice, drivers' behaviour when driving on a rutted road also affects the situation. Stresses in the road's pavement spread to a relatively wide area even with thin surface layers, thus also decreasing displacements.

Most permanent deformations in all the structures occurred in the subgrade sand (47–59%). Permanent deformations in the materials showed a clear increase after a threshold value corresponding to a certain stress state was exceeded. The back-calculated resilient moduli for the sand layer gave results 15–40% lower than the values determined in the laboratory. Contrary to expectations, the back-calculated resilient modulus was the smallest when the load was the greatest and the ground water level lower.

According to radiometric measurements, the water content of the pavements increased approximately 0.2–0.5% units when the ground water level was raised to the top of the subgrade. When the ground water was at the top of the subgrade (-0.5 m from the surface layer) a relatively larger share of permanent deformations occurred in the subbase gravel and the subgrade. When the ground water was lower (-1.0 m) a greater share of displacements occurred higher up in the base course.

The fourth power rule does not apply to low-volume roads. It can be estimated on the basis of the rule that on loading levels 50 to 70 kN and traffic volumes greater than 200 to 400 passes, the design is governed by permanent deformations in the structure, not fatigue.

5.5 Tests 24–29

The rehabilitation of structures tested and rutted in the Low-volume roads study was successful. The structures had rutted and damaged in different ways during the previous tests. Rehabilitation of the structures evened out the differences in the condition of the structures, because after rehabilitation, the bearing capacities measured with a falling weight deflectometer showed no major differences between the structures. The bearing capacities increased significantly in all the structures. In fact, they more than doubled compared to the original situation.

The unreinforced reference structures showed the deepest ruts at the end of the test. Clearly the slowest structure to become rutted was structure 28, which contained the steel grid with 6 mm transverse bars. On the other hand, structure 25, with an identical steel grid, rutted nearly as fast as the unreinforced reference structure 24. The structures on the centremost loading area, with an 8 mm steel grid or fibreglass reinforcement, rutted almost equally fast.

The different rutting behaviour of the various pairs of structures can be explained by the different condition of the structures before rehabilitation, the varying thickness of the asphalt layers and the varying degrees of adhesion between the asphalt layers. The effect of the adhesion between the asphalt layer and the reinforcement on the service life and design of the structures will be the subject of a further study.

It would seem that the thickness of the bars in the steel grid have no effect on rutting speed in this case. In other words, the capacity of the steel grid with thinner bars is great enough to receive the mobilised stress without major deformations. Furthermore, it seems that the worse the condition of the original structure the better the reinforced structure performs.

The earth pressure values for unbound layers showed a clear decrease due to the rehabilitation of the structures. The earth pressure of the gravel layer in the rehabilitated structure decreased 42–58%. The decrease in the earth pressure in the clay layer was slightly less, approximately 38–48%. The structures, where the cross-section was changed in connection with the rehabilitation, showed a smaller decrease in earth pressure than the structures that retained their shape.

These findings can be summarised by saying that using various reinforcements in the rehabilitation of low-volume roads can clearly extend the service life compared to unreinforced rehabilitation. The extension of the service life achieved is case- and site-specific, depending on the condition of the old surface structure, the properties of the rut levelling, the reinforcement used and the new asphalt, but most of all how all of these factors function together. The test results allow us to indirectly estimate that the adhesion of the reinforcement to its base and the new surface layer on the one hand and the mutual adhesion of the old and new surface layers on the other can have a very significant effect on the extension of the service life achieved. Adhesion could be the single most important factor explaining the great relative improvement observed elsewhere – even greater than in this study – in the service life of a road when using reinforcements. Therefore, it is highly advisable to study the effect of adhesion in more detail.

6 REFERENCES

/1/ Elomaa, J. Testing of EPS as Lightweight Fill for Road with the Heavy Vehicle Simulator. Helsinki University of technology. Dept. of Civil and Environmental Engineering. Masters's Thesis (in Finnish) 8.2.2002, 69 p.

/2/ Huurman M., 1997, Permanent deformation in concrete block pavements, Ph.D. thesis, Delft University of Technology, the Netherlands

/3/ Kangas, H., Onninen, H. and Saarelainen, S., *Testing a pavement on thawing, frost-susceptible subgrade with the heavy vehicle simulator.* Helsinki 2000. Finnish Road Administration. Finnra Reports 31/2000 69 p.

/4/ Korkiala-Tanttu, L., Jauhiainen P., Halonen P., Laaksonen R., Juvankoski M., Kangas H. and Sikiö J., *Effect of steepness of sideslope on rutting.* Helsinki 2003. Finnish Road Administration. Finnra Reports 19/2003 40 p. + 17 app.

/5/ Korkiala-Tanttu, L., Laaksonen, R., Törnqvist, J., *Effect of the spring and overload on the rutting of a low-volume road.* HVS-Nordic-research. Helsinki 2003. Finnish Road Administration. Finnra Reports 22/2003 39 p. + app.

/6/ Korkiala-Tanttu, L, Laaksonen, R., *Reinforcement of the edge of a steep-sloped pavement.* Helsinki 2003. Finnish Road Administration. Finnra Reports nro. 38/2003, 50 p. + app.

/7/ Korkiala-Tanttu L., Rathmayer H. and Kangas H., Performance evaluation of a Bi-component geotextile in accelerated pavement test. Seventh International Conference on Geosynthetics 22.9.-27.9.2002 Nice. In print.

/8/ Pihlajamäki, J., Wiman, L., Gustafson, K., *Full Scale Accelerated Tests*. REFLEX-report D4.2, draft 25.2.2002.

7 APPENDICES

Appendix 1. Overview of HVS tests and results

APPENDIX. OVERVIEW OF HVS TESTS AND RESULTS.

Test	Objective	Structure	Pre-load parameters Passes Wheel load, kN Tyre type Temperature Speed	Test parameters Wheel load, kN Tyre pressure, kPa	Rut depth at		First crack at	Remarks
					Passes (pre-run included)	Rut, mm		
FIN11 Reflex03	Bearing capacity test, steel grid reinforcement in crushed rock	50 mm, Asphalt 200 mm, Crushed rock steel grid 5 mm # 75/75 50 mm, Crushed rock 1400 mm Sand	0-20.000 30 kN, bi-directional, unif. lateral load distribution Single 10 °C 12 km/h	60 kN, bi-directional 800 kPa, lateral load distribution	3060 9700 20000 40000 63000 90000 111000	3.6 15.1 27.5 40.1 48.3 54.8 57.9	7500	
FIN12 Reflex03	Bearing capacity test, steel grid reinforcement in crushed rock	50 mm, Asphalt 200 mm, Crushed rock steel grid 6 mm # 150/150 50 mm, Crushed rock 1400 mm Sand	0-20.000 30 kN, bi-directional, unif. lateral load distribution Single 10 °C 12 km/h	60 kN, bi-directional 800 kPa, lateral load distribution	3060 9700 20000 40000 63000 110000 111000	3.8 16.6 28.5 40.5 48.8 59.2 59.1	7500	
FIN13 Reflex03	Bearing capacity test, reference structure	50 mm, Asphalt 250 mm, Crushed rock 1400 mm Sand	0-20.000 30 kN, bi-directional, unif. lateral load distribution Single 10 °C 12 km/h	60 kN, bi-directional 800 kPa, lateral load distribution	2595 9700 20000 39000 60000 68800	8 25.3 36.6 47.8 55.4 57.8	12000	
FIN14	EPS-structure, influence of light-weight material	50 mm, Asphalt 350 mm, Crushed rock steel grid 6 mm # 150/150 100 mm, Crushed rock 200 mm, EPS 1500 mm Sand	0-3.478 20-50 kN, bi-directional Single-dual 10 °C 12 km/h	50 kN, bi-directional 700 kPa, lateral load distribution	278 955 1525 5120 9620 18120 23120	1.7 6.3 9.7 13.8 19.8 26.6 29.8	15000	
FIN15	EPS-structure, influence of light-weight material	50 mm, Asphalt 450 mm, Crushed rock 200 mm, EPS 1500 mm Sand 100 mm, drainage	0-3.478 20-50 kN, bi-directional Single-dual 10 °C 12 km/h	50 kN, bi-directional 700 kPa, lateral load distribution	278 955 1525 5120 9620 18120 23120	1.9 6.5 9.8 14.6 21.3 28.4 31.8	15000	

Test	Objective	Structure	Pre-load parameters Passes Wheel load, kN Tyre type Temperature Speed	Test parameters Wheel load, kN Tyre pressure, kPa	Rut depth at		First crack at	Remarks
					Passes (pre-run included)	Rut, mm		
FIN16	Sloped structure (no slope), influence of the road cross-section and edge effects	50 mm, Asphalt 400 mm, Crushed rock 200 mm, Gravel Bi-component geotextile 1350 mm, Clay 600 mm, Sand	0-250 20 kN, bi-directional Single 10 °C 12 km/h	30, 40, 50 kN, bi-directional 700 kPa	250 1720 7100 8900 12610 14300 16100	1.8 5.2 7.3 8.3 17.4 20.4 27.5	no cracks	
FIN17	Sloped structure (no slope), influence of the road cross-section and edge effects	50 mm, Asphalt 400 mm, Crushed rock 200 mm, Gravel Application class 3 geotextile 1350 mm, Clay 600 mm, Sand	0-250 20 kN, bi-directional Single 10 °C 12 km/h	30, 40, 50 kN, bi-directional 700 kPa Single 10 °C 12 km/h	250 1720 7100 8900 12610 14300 16100	2.9 7.1 9.6 10.9 23.4 28 35.7	No cracks	
FIN18	Sloped structure (slope 1:3), influence of the road cross-section and edge effects	50 mm, Asphalt 400 mm, Crushed rock 200 mm, Gravel Application class 3 geotextile 1350 mm, Clay 600 mm, Sand	0-250 20 kN, bi-directional Single 10 °C 12 km/h	30, 40, 50 kN, bi-directional 700 kPa	250 1720 7100 8900 12500 16100 17900	1.3 7.5 12.9 16.1 22.5 31.6 48.8	16000	
FIN19	Sloped structure (slope 1:1.5), influence of the road cross-section and edge effects	50 mm, Asphalt 400 mm, Crushed rock 200 mm, Gravel Application class 3 geotextile 1350 mm, Clay 600 mm, Sand	0-250 20 kN, bi-directional Single 10 °C 12 km/h	30, 40, 50 kN, bi-directional 700 kPa	250 1720 7100 8900 12500 16100 17900	0.8 6.7 11.9 14.1 21.2 31.5 51	16000	
FIN20	Sloped structure (slope 1:1.5), influence of the road cross-section and edge effects	50 mm, Asphalt 400 mm, Crushed rock 200 mm, Gravel Bi-component geotextile 1350 mm, Clay 600 mm, Sand	0-250 20 kN, bi-directional Single 10 °C 12 km/h	30, 40, 50 kN, bi-directional 700 kPa	250 1720 7100 8900 12500 16100 17900	0.9 8.8 16.7 19.2 26 37.9 61.3	1600	

Test	Objective	Structure	Pre-load parameters Passes Wheel load, kN Tyre type Temperature Speed	Test parameters Wheel load, kN Tyre pressure, kPa	Rut depth at		First crack at	Remarks
FIN21	Low-volume road structure, effect of spring and overload	50 mm, Asphalt 200 mm, Crushed rock 250 mm, Crushed gravel 1500 mm Sand	0-480 20 kN, bi-directional, unif. lateral load distribution Dual ? 10 °C 12 km/h	(0-300, 30-50 kN) 300-> 70 kN, bi-directional, special lateral load distribution 850 kPa	300 700 1100 3550 8650 18850 27000 52500 70060	1.2 8.3 12.5 23.8 33.3 41.6 46.1 55.6 60.1	32 000	GW in the surface of sand layer (W -0.5 m)
FIN22	Low-volume road structure, effect of spring and overload	50 mm, Asphalt 200 mm, Crushed rock 250 mm, Crushed gravel 1500 mm Sand	0-480 20 kN, bi-directional, unif. lateral load distribution Dual ? 10 °C 12 km/h	(0-300, 30-50 kN) 300-> 50 kN bi-directional, special lateral load distribution 700 kPa	300 830 2450 4450 8450 20450 42000 70000	1.4 3.7 6.3 7.9 9.7 12.3 15.1 17.6	no cracks	GW in the surface of sand layer (W -0.5 m)
FIN23	Low-volume road structure, effect of spring and overload	50 mm, Asphalt 200 mm, Crushed rock 250 mm, Crushed gravel 1500 mm Sand	0-480 20 kN, bi-directional, unif. lateral load distribution Dual 10 °C 12 km/h	(0-300, 30-50 kN) 300-> 70 kN, bi-directional, special lateral load distribution 850 kPa	300 850 2890 5340 12070 17990 40020 70006	0.6 3.7 6.4 8 11.3 13.2 18.1 22.1	40000 - 70000	GW 0.5 m below the surface of sand layer (W -1.0 m)

Test	Objective	Structure	Pre-load parameters Passes Wheel load, kN Tyre type Temperature Speed	Test parameters Wheel load, kN Tyre pressure, kPa	Rut depth at		First crack at	Remarks
FIN24	Steep reinforced slope structure (now 1:1.5 slope), structure 16 as rehabilitated	40 mm, Asphalt Reinforcement about 48 mm Asphalt 50 mm, Asphalt 400 mm, Crushed rock 200 mm, Gravel Bi-component geotextile 1350 mm, Clay 600 mm, Sand	0-250 20 kN, bi-directional Single 10 °C 12 km/h	30-50 kN, bi-directional 700 kPa	250 591 3502 8906 17370 24510 32060 39006	0.4 1.3 2 2.6 3.7 5.5 7.8 10.5	no cracks	No reinforcement
FIN25	Steep reinforced slope structure (now 1:1.5 slope), structure 17 as rehabilitated	40 mm, Asphalt Reinforcement about 48 mm Asphalt 50 mm, Asphalt 400 mm, Crushed rock 200 mm, Gravel Application class 3 geotextile 1350 mm, Clay 600 mm, Sand	0-250 20 kN, bi-directional Single 10 °C 12 km/h	30-50 Kn, bi-directional 700 kPa	250 591 3502 8906 17370 24510 32060 39006	0.4 1.3 2 2.7 3.5 5.1 6.9 8.8	no cracks	B500H - 5/6 - 200/150 steel grid
FIN26	Steep reinforced slope structure (now 1:1.5 slope), structure 18 as rehabilitated	40 mm, Asphalt Reinforcement about 85 mm Asphalt 50 mm, Asphalt 400 mm, Crushed rock 200 mm, Gravel Application class 3 geotextile 1350 mm, Clay 600 mm, Sand	0-250 20 kN, bi-directional Single 10 °C 12 km/h	30-50 kN, bi-directional 700 kPa	250 597 3516 8920 17390 24530 35330 39000	0.4 1.1 1.7 2.4 3.2 4.2 6.1 6.8	no cracks	B500H - 5/8 - 200/150 steel grid

Test	Objective	Structure	Pre-load parameters Passes Wheel load, kN Tyre type Temperature Speed	Test parameters Wheel load, kN Tyre pressure, kPa	Rut depth at		First crack at	Remarks
FIN27	Steep reinforced slope structure (now 1:1.5 slope), structure 18 as rehabilitated	40 mm, Asphalt Reinforcement about 85 mm Asphalt 50 mm, Asphalt 400 mm, Crushed rock 200 mm, Gravel Application class 3 geotextile 1350 mm, Clay 600 mm, Sand	0-250 20 kN, bi-directional Single 10 °C 12 km/h	30-50 kN, bi-directional 700 kPa	250 597 3516 8920 17390 24530 32070 39000	0.3 0.9 1.4 1.9 2.9 4.4 5.1 6.6	no cracks	Fibreglass grid Polyfelt PGM-G100/100
FIN28	Steep reinforced slope structure (1:1.5 slope), structure 19 as rehabilitated	40 mm, Asphalt Reinforcement about 98 mm Asphalt 50 mm, Asphalt 400 mm, Crushed rock 200 mm, Gravel Application class 3 geotextile 1350 mm, Clay 600 mm, Sand	0-250 20 kN, bi-directional Single 10 °C 12 km/h	30-50 kN, bi-directional 700 kPa	250 560 3480 8881 17330 24480 35300 38960	0 0.6 0.8 1.2 1.8 2.5 4.8 5.3	no cracks	B500H - 5/6 - 200/150 steel grid
FIN29	Steep reinforced slope structure (1:1.5 slope), structure 20 as rehabilitated	40 mm, Asphalt Reinforcement about 98 mm Asphalt 50 mm, Asphalt 400 mm, Crushed rock 200 mm, Gravel Bi-component geotextile 1350 mm, Clay 600 mm, Sand	0-250 20 kN, bi-directional Single 10 °C 12 km/h	30-50 kN, bi-directional 700 kPa	250 560 3480 8881 17330 24480 35300 38960	0 0.8 1.2 1.9 2.5 3.7 7 7.8	no cracks	No reinforcement

ISSN 1459-1553
ISBN 951-803-127-4
TIEH 3200832E-v